

Inhibiting ethylene perception with 1-methylcyclopropene triggers molecular responses aimed to cope with cell toxicity and increased respiration in citrus fruits

5 Beatriz Establés-Ortiz, Paco Romero, Ana-Rosa Ballester, Luis González-Candelas, María T. Lafuente*

Instituto de Agroquímica y Tecnología de Alimentos (IATA-CSIC). Consejo Superior de Investigaciones Científicas. Av. Agustín Escardino, 7. 46980, Paterna-Valencia, Spain.

10

Beatriz Establés-Ortiz, bestables@gmail.com

Paco Romero, ciepro@iata.csic.es

Ana-Rosa Ballester, ballesterar@iata.csic.es

Luis González-Candelas, lgonzalez@iata.csic.es

15 *Corresponding author: María-Teresa Lafuente, mtlafuente@iata.csic.es; Telephone: +34-963900022; FAX: +34-963636301

20 ABSTRACT

The ethylene perception inhibitor 1-methylcyclopropene (1-MCP) has been critical in understanding the **hormone's mode of action**. However, 1-MCP may trigger other processes that could vary the interpretation of results related until now to ethylene, which we aim to understand by using transcriptomic analysis. Transcriptomic changes in ethylene- and 1-MCP-treated 'Navelate' (*Citrus sinensis* L. Osbeck) oranges were studied in parallel with changes in ethylene production, respiration and peel damage. The effects of compounds modifying the levels of the ethylene co-product cyanide and nitric oxide (NO) on fruit physiology were also studied. Results suggested that: 1) The ethylene treatment caused sub-lethal stress since it induced stress-related responses and reduced peel damage; 2) 1-MCP induced ethylene-dependent and ethylene-independent responsive networks; 3) 1-MCP triggered ethylene overproduction, stress-related responses and metabolic shifts aimed to cope with cell toxicity, which mostly affected to the inner part of the peel (albedo); 4) 1-MCP increased respiration and drove metabolism reconfiguration for favoring energy conservation but up-regulated genes related to lipid and protein degradation and triggered the over-expression of genes associated with the plasma membrane cellular component; 5) Xenobiotics and/or reactive oxygen species (ROS) might act as signals for defense responses in the ethylene-treated fruit, while their uncontrolled generation would induce processes mimicking cell death and damage in 1-MCP-treated fruit; 6) ROS, the ethylene co-product cyanide and NO may converge in the toxic effects of 1-MCP.

KEYWORDS

Ethylene, 1-methylcyclopropene (1-MCP), non-climacteric fruits, oxidative stress, respiration, xenobiotics.

45

1. INTRODUCTION

The hormone ethylene plays important roles in development, fruit ripening, abscission, senescence and stress (Abeles et al., 1992). The ethylene signalling pathway and the responses related to the hormone in stressed plants and climacteric fruits have been widely investigated. Less information exists concerning non-climacteric fruits (Wang et al., 2010). The discovery of 1-methylcyclopropene (1-MCP) as a specific inhibitor of ethylene, counteracting ethylene at the receptor level, was a critical breakthrough in understanding the diverse roles of the hormone in plants and also in fruits (Watkins, 2006). As a gas, 1-MCP offers the possibility of facile and uniform delivery, even to bulky plant organs. Therefore, 1-MCP has been especially relevant in research done in fruits from woody plants, where artificially generated mutants are uncommon. Nevertheless, there is a general consensus within the scientific community regarding the fact that 1-MCP may induce additional mechanisms to those regulated by ethylene that may be relevant for the interpretation of results derived from 1-MCP application when studying the diverse roles of ethylene. These mechanisms are still unknown in site of the nearly 20 years that have passed since 1-MCP was discovered and the huge number of studies performed using 1-MCP. None of these studies considered additional effects of 1-MCP.

Different reports suggest that the production of new ethylene receptors may be responsible for the loss of efficacy of 1-MCP blocking the perception of ethylene (Prange et al., 2005); that 1-MCP may be metabolized in plants (Huber et al., 2010); and that ethylene and 1-MCP may bind with different affinities to different ethylene receptors (Cools et al., 2011). The situation is not simple because the effects of 1-MCP, like those of ethylene, differ among species and depend on the physiological stage. Moreover, 1-MCP may have contrary effects, either reducing or enhancing physiological disorders. Two examples are the 1-MCP-induced reduction of postharvest superficial scalding in apples, which produce high ethylene levels (Watkins, 2006), and the 1-MCP-induced increase in postharvest peel damage disorders in citrus fruits, which produce very low hormone levels (Lafuente and Sala, 2002; Lafuente et al., 2001). These differences might be related to the effect of ethylene on the mechanisms operating in the development of such disorders, but we cannot exclude the different

effect of 1-MCP on the biosynthesis of ethylene and its co-products as well as on its
80 associated responses in such fruits.

Mature non-climacteric citrus fruit evolves very low amounts of ethylene, but ethylene sharply increases in response to stress and following inhibition of its perception because this fruit displays autoinhibitory ethylene production (Lafuente et al., 2001; Marcos et al., 2005; McCollum and Maul, 2007). Responses to ethylene
85 include induction of ripening-related changes, accelerated respiration and activation of stress-defense responses (Gonzalez-Candelas et al., 2010; John-Karuppiah and Burns, 2010; McCollum and Maul, 2007). Previous investigations suggest a link between carbon starvation stress and the 1-MCP-induced rises in respiration and peel damage in detached mature citrus fruit (Cajuste et al., 2011), and show that conditioning citrus
90 fruits with ethylene reduces this disorder known as non-chilling peel pitting (NCP) (Supplementary Fig. S1A) (Lafuente and Sala, 2002). The symptoms of NCP are collapsed areas of part of the albedo (inner part of the peel) and the flavedo (outer colored part), which may become brown with time if the severity of the disorder is very high. 1-MCP should block protective mechanisms induced by the hormone or modify its
95 interaction with other molecules and pathways in the complex network of regulatory defense responses. These reasons, in addition to the fact that 1-MCP increases endogenous ethylene in citrus fruit, make mature citrus fruit a good experimental system for studying whether 1-MCP has additional effects to those regulated by the hormone.

100 Genomic tools have been quickly adopted to address major challenges of citrus fruit. Yet only one comprehensive transcriptomic study has been performed to determine the effect of ethylene in the flavedo of still green fruits (Fujii et al., 2007). This study used very high ethylene levels ($100 \mu\text{L L}^{-1}$) and focused on the mechanisms occurring during the conversion of chloroplast to chromoplast during degreening. Physiological
105 responses to ethylene, however, are influenced by the maturity stage in citrus fruit (John-Karuppiah and Burns, 2010). Transcriptomic studies have been also performed to study the role of ethylene in the regulation of citrus peel genes induced by fungal infection (Gonzalez-Candelas et al., 2010). However, no large-gene expression analysis has been conducted yet comparing the responses of the albedo and the flavedo to
110 ethylene and 1-MCP and their effects in detached mature fruits.

Our working hypothesis was that 1-MCP, besides inhibiting ethylene action, may regulate complex mechanisms related to ethylene co-products and/or to increased

respiration and that such mechanisms might favor, in part, stress that may end in peel collapse in harvested mature citrus fruit. To test this hypothesis, and to compare such mechanisms with those induced by ethylene concentrations that reduce peel collapse, we have investigated the effects of ethylene and 1-MCP at the transcriptomic level. Transcriptome analysis of the flavedo and the albedo was performed because both tissues are highly affected by NCPP (Cajuste et al., 2011) and their morphology and ability to provide energy is different (Matas et al., 2011). Moreover, previous research from our group showed that structural and histochemical changes induced by ethylene were more marked in the albedo (Cajuste et al., 2011). Considering results from the transcriptomic analysis, we further examined whether cyanide, stoichiometrically co-produced during ethylene biosynthesis (Peiser et al., 1984), and nitric oxide (NO) may mimic the postharvest NCPP syndrome, and whether inhibiting or scavenging cyanide or NO may reduce the deleterious effect of 1-MCP.

2. MATERIALS AND METHODS

2.1. Plant material and treatments

‘Navelate’ sweet oranges (*Citrus sinensis* L. Osbeck) were harvested 3 months after color change from adult trees in Castellón, Spain. The oranges were immediately divided into three groups containing an equal number of fruits and exposed to the following treatments: continuous flow of air after being conditioned with 10 $\mu\text{L L}^{-1}$ ethylene for 4 days (EC, group 1); continuous flow of air (AC, group 2); continuous flow of air after being treated with 1 $\mu\text{L L}^{-1}$ 1-MCP for 14 h (group 3) (Fig. 1). All the treatments were performed in sealed containers, which were kept in controlled temperature and humidity storage rooms, and in the presence of $\text{Ca}(\text{OH})_2$ to prevent the accumulation of respiratory CO_2 . Fruits were always kept at 20 °C and 90–95% relative humidity (RH) to avoid environmental stress. 1-MCP, donated by Rohm and Haas Spain, S.A., was prepared and fumigated following the manufacturer’s instructions. Fruits from each group were ventilated after fumigation and randomly divided into 3 replicates of 10 fruits to estimate ethylene production, respiratory rate and NCPP index. Additional replicate samples of 5 fruits per treatment and storage period and of freshly harvested fruits were used for transcriptomic analysis. Transcriptomic data were

gathered from freshly harvested fruits and from air control (AC), EC and 1-MCP-treated oranges held for 4 and 14 days at 20 °C. The experimental design, outlined in Fig. 1, was established to focus on short- (4 days) and long-term (14 days) responses induced after 1-MCP application and also to compare these responses with those induced by ethylene at day 4 since the 4 days of EC treatment showed a high efficacy in reducing NCPP. Although transient changes in gene expression might be induced by ethylene at 20 °C in a few hours, it is important to note previous results from our group showing that the high efficacy of the EC treatment is reduced when the treatment is shortened (Lafuente and Sala, 2002). These initial transient responses would be also induced by the shorter treatments in spite of their lower efficacy. Therefore, the effectiveness of the EC treatment was not limited to transient responses induced during the ethylene treatment. Taking into account this, our experimental design focused on initial responses induced by ethylene that persisted for at least 4 days and on other secondary responses occurring by day 4. These responses should be especially relevant for the persistence of the efficacy of the EC treatment. Moreover, the incidence of peel collapse sharply increased after 4 days in the 1-MCP-treated fruits. At this time point differences in NCPP between the control CA fruits and the 1-MCP-treated fruits started to be apparent. The 14 days period was selected to further know the long-term 1-MCP-induced responses. This approach also allowed focusing on mechanisms occurring in fruits exposed for prolonged periods to the high ethylene levels produced by the 1-MCP-treated fruits, or related to putative co-products generated during hormone biosynthesis or to the increased respiration. Harvested fruits treated for 4 days with the hormone were transferred to air for 10 additional days to compare long-term responses induced by day 14 in 1-MCP-treated and the EC-treated fruits, respect to their control sample held for 14 days in air (control fruit, AC). Similarly, changes induced at day 4 by ethylene were compared with those occurring in AC and 1-MCP-treated fruits (Fig. 1). The flavedo and the external layer of the albedo were collected periodically from the total fruit surface, immediately frozen and grounded in liquid nitrogen and stored at -80 °C. Three biological replicates originate from different sample sets coming from three independent experiments performed in different citrus seasons were collected at each sampling period and used for each analysis.

2.2. Feeding experiments

180 For each treatment, 3 replicates of 10 fruits were used. Fruits were dipped for 2
min in different solutions (1 μ M, 10 μ M, 100 μ M and 1 mM) of sodium nitroprusside
(SNP), 300 μ M hydroxocobalamin (HB), 300 μ M 2-[4-carboxyphenyl],4,4,5,5-
tetramethylimidazoline-1-oxy-3-oxide (cPTIO) or de-ionized water. Fruits treated with
HB and cPTIO were treated with 1-MCP following the same procedure described
185 above. All the fruits were then stored in the dark at 20 °C and 90–95% RH. All
chemicals were from Sigma–Aldrich (St. Louis, MO, USA).

2.3. Ethylene production and respiratory rate determination

190 Ethylene production from whole fruits was measured periodically by incubating 3
replicate samples of 10 fruits in 3 L sealed glass jars at 20 °C for 3 h. Ethylene samples
were withdrawn from each jar and injected into a gas chromatograph, equipped with an
activated alumina column and a flame ionization detector (Lafuente et al., 2001). The
respiratory rate was determined by measuring CO₂ production. CO₂ evolution was
195 determined following the same procedure but using a Chromosorb 102 column and a
thermal conductivity detector (Cajuste et al., 2011).

2.4. Estimation of nonchilling peel pitting damage

200 A visual rating scale was used to estimate the extent of NCPP development
(Supplementary Fig. S1). This scale was established on the basis of surface damage and
ranged from 0 (no damage) to 4 (severe damage). The average NCPP index was
calculated according to Lafuente and Sala (2002), and the results are the means of the
three replicate samples \pm SE.

205

2.5. RNA isolation and preparation of labelled cDNA probes

Total RNA was isolated from flavedo and albedo tissues, its concentration was
measured spectrophotometrically, and its integrity verified by agarose gel
210 electrophoresis and ethidium–bromide staining (Ballester et al., 2011). Processing of
RNA samples for microarray hybridizations, reverse transcription, cDNA purification,
dye coupling, and fluorescent cDNA purification were performed according to Ballester

et al. (2011). Three biological replicates were used for RNA isolation and the subsequent microarray hybridization and validation by RT-qPCR.

215 2.6. Microarray hybridization, data acquisition and data analysis

A 12k citrus cDNA microarray developed by the Spanish Citrus Functional Genomic Project (CFGP, <http://bioinfo.ibmcp.upv.es/genomics/cfgpDB/>) (Martinez-Godoy et al., 2008) was used. The microarray contains 24,288 probes corresponding to
220 11,241 putative unigenes from citrus, which constitutes a high representation of the citrus genome. Of these genes, 77.1% have an *A. thaliana* homolog (Ballester et al., 2011). Microarray hybridization and scanning were performed as described by Ballester et al. (2011). Samples were hybridized against a reference sample containing a mix of equal amounts of RNA of all the experimental samples. The use of this reference
225 sample has been widely used in *Citrus* transcriptomic research since represent a powerful tool for reducing the number of hybridizations to make all the possible pairwise comparisons between samples (Ballester et al., 2011; Romero et al., 2012). SAM (Significant Analysis of Microarrays), included in the TM4 Microarray Software Suite, was used to identify differentially expressed genes using a False Discovery Rate
230 threshold p -value<0.01 as previously described (Ballester et al., 2011; Romero et al., 2012). FatiGO+ (Babelomics, <http://babelomics.bioinfo.cipf.es>) was used to identify processes that were significantly over- or under-represented in a particular set of differentially expressed genes relative to a reference group composed of all genes in the microarray with an *Arabidopsis thaliana* homolog (Ballester et al., 2011; Romero et al.,
235 2012). Gene ontology analysis for induced and repressed genes was independently performed applying a Fisher two-tailed test (p -value<0.05). Transcriptomic data were also loaded into MapMan (<http://www.gabipd.de/projects/MapMan/>) to visualize the gene expression data on a metabolic map (Thimm et al., 2004).

240 2.7. RT-qPCR expression analysis

Reverse transcription of flavedo and albedo RNA samples followed by quantitative polymerase chain reaction analysis (RT-qPCR) was performed to validate microarray results as previously described by Romero et al. (2012). The LightCycler
245 SW 1.5 software was used and a two-step RT-qPCR assay designed. Forward (F) and

reverse (R) sequences for selected primers and reference genes used for data normalization, whose constitutive expression was confirmed by using the geNorm program, are summarized in Supplementary Table S1. Statistical analysis (Pair Wise **Fixed Reallocation Randomisation Test**) was performed by the $\Delta\Delta Ct$ method using the Relative Expression Software Tool (REST, <http://rest.gene-quantification.info/>). Each biological replicate sample was analyzed in duplicate.

2.8. Statistics

A mean comparison using Tukey's test and Statgraphics.5.1 Software was performed to determine significant differences ($p \leq 0.05$) in NCPP, ethylene production and the respiratory rate.

3. RESULTS

260

3.1. 1-MCP triggers a maintained ethylene overproduction and enhances respiration and peel collapse in citrus fruit

The 1-MCP treatment had a more marked effect on increasing ethylene levels than the ethylene applied during the EC treatment (Fig. 2A). During the first day of hormone treatment the endogenous ethylene level of the fruits was barely modified, but it increased 3-fold by day 2 and remained high until the fruits were transferred to air (Fig. 2A, insert panel). 1-MCP led to a sharp increase in hormone levels, reaching a maximum by day 7 (Fig. 2A). At this time point, a ca. 200-fold ethylene increase was observed. Ethylene production decreased thereafter, but it was still much higher than in control fruits. The 1-MCP-induced rise in CO_2 was much lower (ca. 3-fold increase) (Fig. 2B). Detachment and continuous holding of oranges in air under non-stressful environmental conditions (AC fruits) induced the development of NCPP symptoms after 3 days (Fig. 2C). The incidence of the disorder was lower in the EC fruits and enhanced by the 1-MCP treatment. This trend, as well as that of ethylene production, was confirmed in fruits harvested in a second citrus season.

270

275

3.2. 1-MCP and ethylene elicit common but also different transcriptional profiles

280 Global gene expression was analyzed in EC, AC and 1-MCP-treated fruits and compared to that of freshly harvested fruits according to the experimental design described above and outlined in Fig. 1. The number of differentially expressed genes is summarized in Fig. 3. SAM analysis revealed major changes in fruits treated for 4 days with ethylene and at long-term (14 days) in the 1-MCP-treated fruits. The largest differences were observed by day 14 in the albedo of the 1-MCP-treated fruits. The number of ethylene-induced genes (4 days) decreased considerably after transferring the fruits to air. In contrast, the number of up-regulated genes increased more than 10-fold between 4 and 14 days in the 1-MCP-treated fruits. The sensitivity and consistency of the microarray analysis was confirmed by determining the expression of selected genes (Supplementary Table S1) using RT-qPCR. Results showed a high correlation ($r^2 = 0.807$, $p \leq 0.05$) between the microarray and the RT-qPCR results (Supplementary Fig. S2).

295 Differentially expressed genes were classified into biological processes that were clustered according to their over-/infra-representation either in the albedo or the flavedo of fruits treated with ethylene or 1-MCP (Table 1). As explained above, both tissues are highly affected by NCPP and they show different ability to provide energy, and also different structural and histochemical changes in response to ethylene. Therefore, results from both tissues are complementary. No biological process was over- or infra-represented after short-term (4 days) in the 1-MCP-treated fruits (Table 1). Pattern 1 in Table 1 includes processes induced only at long-term in the 1-MCP-treated fruits and pattern 2 processes that might be counteracted by 1-MCP. Processes related to the defense response to pathogens prevailed within pattern 1, although other processes involving abiotic stresses and response to toxins were also over-represented. Processes related to fatty acid biosynthesis prevailed in pattern 2. Other processes were over-represented at long-term in the 1-MCP-treated fruits and induced at day 4 by ethylene (pattern 3); while processes within pattern 6 were counteracted by ethylene and 1-MCP. Ethylene specifically repressed photosynthesis-related processes and induced processes related to lignin biosynthesis in the albedo and flavedo (pattern 4). Other processes like **‘response to hypoxia’ were only over-represented in the albedo. The ‘oxylipin metabolic process’**, which included abundant genes encoding lipoxygenases (LOX), was the only

300
305
310

over-represented process that persisted at long-term after fruit transference to air. By day 14, expression levels of these *LOX* genes were in general lower in the 1-MCP-treated fruit (Supplementary Table S2). Processes within pattern 5 might be counteracted by ethylene and **belonged to general GO levels, except the ‘response to jasmonic acid stimulus’**. Gene ontology analysis also revealed that, at long-term, 1-MCP induced molecular functions related to serine/threonine and tyrosine kinase activity and to ATP binding (Table 2). Molecular functions over-represented specifically in the EC fruits showed oxidoreductase, UDP-glycosyltransferase and **nucleotide kinase activities. Moreover, the ‘kinase activity’ and the ‘heme and iron ion binding’ functions were induced by both ethylene and 1-MCP.** Both treatments infra-represented **the ‘thylakoid membrane’ cellular component in the albedo, although this effect was reversed after transferring EC fruit to air (Table 2).** Moreover, the over-expression of genes associated with the **‘plasma membrane’ component only occurred at long-term in this tissue in response to 1-MCP.** The study of protein domains (InterPro Table 2) further indicated the relevance of protein phosphorylation at long-term in the 1-MCP-treated fruits and of proteins containing *LOX* domains in EC fruits by day 14.

3.3. *1-MCP-induced metabolism alteration in the peel of citrus fruit*

To better visualize the gene expression data on a metabolic map, transcriptomic data were analyzed with MapMan. Little changes were found by day 4 in the albedo and the flavedo of the 1-MCP-treated fruits respect to control fruits (data not shown). Changes in the transcript levels in the albedo of the 1-MCP-treated fruits (14 days) have been highlighted in this paper (Fig. 4) since major changes were observed in this sample. 1-MCP favored the repression of genes involved in starch synthesis and degradation and increased the expression levels of sucrose synthase genes involved in sucrolysis via the sucrose pathway and of genes encoding cell wall hydrolases. The ethylene antagonist also favored the up-regulation of glycolytic genes and of genes within the fermentative anaerobic pathway, which fits with the induction of other genes within **the biological process ‘response to hypoxia’** (Supplementary Table S2). The most important change within this process corresponded to the gene encoding hemoglobin II, whose expression increased 8-fold. Moreover, 1-MCP up-regulated **genes encoding lipases and esterases and participating in lipid β -oxidation** and in amino acid and protein catabolism (Fig. 4). 1-MCP also raised the expression of genes

345 involved in mitochondrial electron transport and of cytochrome P450 and ATP synthase-encoding genes. In contrast, 1-MCP barely affected the alternative respiration pathway and slightly repressed the mitochondrial uncoupling protein (UCP) pathway (Fig. 4).

350 Among genes within the TCA-cycle, the most relevant inductions corresponded to those coding for aconitase and isocitrate dehydrogenase. These genes participate not only in cell energetics but also in the generation of intermediates leading to nitrogen assimilation via amino acid biosynthesis by the concerted action of glutamine synthase (GS) and glutamate 2-oxoglutarate aminotransferase (GOGAT) in the GS/GOGAT cycle, which was activated by 1-MCP. In concordance with this result, 1-MCP had, at
355 long-term, an important effect on activating the chorismate and the subsequent phenylpropanoid pathways (Fig. 4), and this effect was more marked than in EC fruit (4 days, data not shown). Transcriptomic data further showed that 1-MCP down-regulated genes associated with light reaction centers and the Calvin cycle and up-regulated oxidative stress-related genes (Fig. 4).

360

3.4. 1-MCP up-regulates at long-term genes involved in ethylene biosynthesis and perception and in cyanide and reactive oxygen species (ROS) detoxification

Changes in fruit endogenous ethylene levels and the examination of genes within
365 **the process ‘response to toxin’** (Supplementary Table S2) suggested that overproduction of ethylene and/or cyanide, which is stoichiometrically co-produced during ethylene biosynthesis from 1-aminocyclopropane-1-carboxylic acid (ACC), may contribute to higher NCPP in the 1-MCP-treated fruits. To verify this, and to further investigate whether some of the 1-MCP-induced transcriptional profiles found in the albedo and the
370 flavedo may be related to ethylene overproduction, changes in the expression of genes printed in the microarray related to ethylene biosynthesis, perception and signalling, and also to cyanide detoxification, were examined in the peel (Table 3). Major changes were found in ACC oxidase (ACO)-encoding genes and ACC oxidase oxidizes ACC to ethylene and cyanide. Some of them are still annotated as ethylene-forming enzymes in
375 the *Arabidopsis* database. These changes were, in general, higher in the albedo of the 1-MCP-treated fruits. Furthermore, ethylene and 1-MCP treatments modulated genes involved in ethylene perception and signal transduction. From a total of 4 genes encoding ethylene receptors printed in the microarray, 2 were induced at long-term in

the 1-MCP-treated fruits. Likewise, ethylene (4 days) and 1-MCP (14 days) modulated
380 ethylene-responsive factors. Only 1-MCP **was able to induce the ‘response to ethylene
stimulus’** (Supplementary Table S2). Although transient responses induced initially by
either ethylene or 1-MCP were not determined, these results suggest that some
responses induced by 1-MCP at long-term are indeed regulated by ethylene.

Expression levels of the genes involved in cyanide detoxification were clearly
385 higher in the 1-MCP-treated fruits by day 14 (Table 3). Major expression levels were
observed in a β -cyanoalanine synthase (CAS)-encoding gene, whereas this gene was
down-regulated in the 1-MCP-treated fruits by day 4. Its expression was lower in the 1-
MCP-treated fruits (14 days) than in the EC fruits (4 days). Therefore, the ability of 1-
MCP-treated fruits to detoxify cyanide should be lower. Two of these cyanide
390 detoxifying genes **belonged to the ‘response to toxin’ process**, which is relevant for
xenobiotic and ROS detoxification and mostly groups genes encoding glutathione
transferases (GSTs) (Supplementary Table S2). MapMan visualization of transcriptomic
data also suggested that 1-MCP favor oxidative stress. Considering that an excess of
ethylene and/or cyanide may favor ROS in plants (Munné-Bosch et al., 2004; Oracz et
395 al., 2009), we further focused on transcriptomic data related to generation and
detoxification of ROS. Ethylene modulated genes involved in oxidative stress, but
major changes were observed by day 14 in the 1-MCP-treated fruits. Besides the high
representation of *GSTs*, we observed the induction of the blue copper oxidases,
annotated as dicyanins, and of genes in the ascorbate-glutathione cycle (Supplementary
400 Table S3). Genes leading to the detoxification of ROS within the thioredoxin-dependent
pathway or favoring H_2O_2 formation, such as those encoding glycolate and amine
oxidases, were also mostly induced at long-term by 1-MCP (Supplementary Table S3).
Furthermore, 1-MCP activated protein serine/threonine kinase cascades (Table 2) and
up-regulated oxidative genes like CPR2 or nectarin, whose expression increased more
405 than 16- and 32-fold in the albedo, respectively. Likewise, data summarized in Table 4
showed that 1-MCP induced a high representation of genes involved in detoxification or
in response to toxin in the albedo (Riechers et al., 2010). Many of these genes have been
related to safeners (Riechers et al., 2010) or to nitric oxide (NO) (Arasimowicz and
Floryszak-Wieczorek, 2007), which can partly mediate some of the effects of cyanide
410 (Bethke et al., 2006).

3.5. *1-MCP-induced damage is reduced by inhibiting cyanide or scavenging nitric oxide*

415 To further test whether cyanide can participate in the detrimental effect of 1-MCP, fruits were treated with SNP, which releases cyanide and NO. Therefore, SNP offers the possibility of testing the involvement of both molecules in 1-MCP-mediated toxicity. The effect of HB, which binds cyanide to form harmless cyanocobalamin, and of the NO scavenger cPTIO on the incidence of damage in 1-MCP-treated fruit was also
420 examined. SNP mimicked the NCPP syndrome (Supplementary Fig. S1) in a dose-dependent manner (Fig. 5A). Moreover, both HB and cPTIO reduced NCPP in the 1-MCP-treated fruits (Fig. 5B) and had little effect on control fruits (data not shown). These results, together with the fact that HB and cPTIO did not modify endogenous ethylene levels (Supplementary Fig. S3), indicate that the 1-MCP-induced ethylene co-
425 product cyanide and NO may modulate additional responses to those regulated by the hormone and that these molecules may be involved in the peel damage associated with the 1-MCP treatment.

4. DISCUSSION

430 Results revealed that 1-MCP triggers, after 4 days, a maintained ethylene overproduction and a marked but lower increase in respiration in citrus fruit, and that changes in gene expression triggered by day 4 by 1-MCP were less relevant than those triggered at long-term. Moreover, results revealed that the long-term responses involve metabolic shifts aimed to cope with cell toxicity and extra energy demand in the peel of
435 detached non-photosynthetic sink mature citrus fruits. These results indicate that 1-MCP regulates complex secondary stress-related responses associated with overproduction of ethylene and its co-products and/or with increased respiration that may end in peel damage.

The fact that 1-MCP up-regulated at long-term **genes involved in β -oxidation** and lipolysis (Fig. 4) is remarkable. This metabolic reconfiguration could be caused by the
440 combination of fruit detachment and extra energy demand associated with the 1-MCP-induced respiratory rise. This energy stress would be complicated by the fact that 1-MCP inhibited the photosynthetic machinery (Fig. 4) that coordinates energy metabolism and balances cell redox status. Extra energy can be obtained from lipid

445 catabolism, and it is known that a respiratory burst is accompanied by a switch in
substrate from carbohydrates to lipids (Theologis and Laties, 1981). Moreover, 1-MCP
favored protein degradation (Fig. 4), which suggests protein utilization as an additional
energy resource. Therefore, lipid and protein degradation might lead to membrane
450 deterioration, as it has been observed in 1-MCP-treated oranges (Cajuste et al., 2011),
and ultimately to damage. Interestingly, plasma membrane was the only cellular
component over-represented at long-term in the albedo of the 1-MCP-treated fruit
(Table 2). Likewise, results suggesting that 1-MCP might favor the sucrose synthase
pathway fit with the carbon economy and imbalance between carbohydrate import and
demand in plants lacking carbohydrate supply. The importance of the interplay between
455 energy status sensing and oxygen availability in the optimization of plant metabolism
should be also kept in mind. In this regard, 1-MCP up-regulated genes involved in
fermentation, which may be induced by a drop in plant energy status (Zabalza et al.,
2009), and up-regulated low oxygen sensors, including hypoxia-responsive genes and
genes involved in trehalose-6-phosphate metabolism (Fig. 4) (Bailey-Serres et al.,
460 2012). Major hypoxia-related responses occurred in the albedo, in agreement with its
lower capacity to provide energy with respect to the flavedo (Matas et al., 2011) and
with the lower environmental oxygen availability in the inner part of the peel.
Therefore, extra energy demand induced by 1-MCP might contribute to the increased
damage in the peel of citrus fruits. Nevertheless, results from this study suggest a higher
465 influence of ethylene overproduction and the associated toxic molecules than the higher
energy requirements of 1-MCP-treated fruits on damage development. This might be
related in part to the fact that the 1-MCP-induced rise in ethylene was much higher than
the rise in respiration.

Physiological data revealed that endogenous ethylene levels increased during fruit
470 exposure to exogenous ethylene, that ethylene production of the EC fruits was lower
than that of the control AC fruits after fruit transference to air, and that the hormone
increase induced by exogenous ethylene was much lower than that induced by 1-MCP.
Ethylene production increases in response to stresses in non-climacteric citrus fruit.
Since the EC treatment reduced postharvest NCPP, and ethylene negatively regulates its
475 own biosynthesis in citrus fruit, the observed increase in hormone biosynthesis during
the EC treatment indicates that the exogenous ethylene levels used were high enough to
produce non-lethal stress. In fact, ethylene induced stress-related responses that might
be involved in cross-protective mechanisms participating in NCPP reduction. The

hormone thus induced responses related to lignin biosynthesis and to the **'oxilypin**
480 **metabolic' process, which participates in the containment of** lesion propagation in
stressed tissues. Furthermore, shortening the ethylene treatment results in a lower NCPP
reduction (Lafuente and Sala, 2002).

In line with the idea that EC produces sub-lethal stress, 1-MCP induced after 4 days
a maintained high non-physiological ethylene overproduction and favored NCPP. As
485 ethylene is perceived at long-term by the fruit because of the synthesis of new ethylene
receptors, this huge ethylene production could lead to damage. The long-term 1-MCP-
induced responses within pattern 3 (Table 1) should be mediated by ethylene, although
these responses were not sufficient to avoid damage. Initial responses induced
immediately after 1-MCP application were not determined, and no biological process
490 was specifically induced by day 4, but the nature of other responses expressed only in
the 1-MCP-treated fruits by day 14 indicates that 1-MCP produces severe stress and that
this stress might be caused by the excess of ethylene and/or its co-product cyanide.
Changes in the expression of cyanide detoxifying genes (Table 3) suggested that the
ability of 1-MCP-treated fruits to detoxify cyanide should be lower. This, together with
495 results showing that the expression of ACO-encoding genes and ethylene production
were much higher in this sample, further suggests that an excess of cyanide may
contribute to the harmful effect of 1-MCP.

Ethylene causes the disruption of chloroplast integrity in green citrus peel (Purvis,
1980). The chloroplast is a major site of ROS production, and severe stress-induced
500 changes in its redox state may trigger programmed cell death (PCD). The effect of the
hormone on mature fruits, where chloroplast has been transformed to chromoplast, is
lesser-known. Results show that ethylene treatment led to an infra-representation of the
'thylakoid membrane' component (Table 2) and **down-regulated the 'photosynthesis'**
process (Table 1). These changes did not persist after transferring EC fruit to air.
505 Results further showed that 1-MCP has at long-term an important effect on the
thylakoid membrane, photosynthesis and light reaction-related genes of the PSII and
PSI centers (Fig. 4 and Supplementary Table S2). These changes resemble
photorespiration energy-sensing responses. Balanced excitation of both PSs is required
for avoidance of oxidative stress and subsequent PCD (Asada, 2006). Therefore,
510 ethylene overproduction for prolonged periods might cause damage in plastids and
favor ROS. This is in concordance with changes in the expression of oxidative stress-
related genes (Supplementary Table S3). These changes, together with the reported

H₂O₂-induced responses in plants (Van Breusegem and Dat, 2006), further suggest that H₂O₂ may lead to PCD induction in citrus fruits that over-produce ethylene. The hydroxyl and ¹O₂ radicals could also contribute to the harmful effect of 1-MCP. These radicals are triggered by PSII inhibition or by dicyanins in the presence of cyanide (Asada, 2006; Van Breusegem and Dat, 2006), and dicyanins were highly induced at long-term by 1-MCP (Supplementary Table S3). Furthermore, 1-MCP at long-term up-regulated a high number of *GSTs* (Table 4). Although the primary function of *GSTs* is xenobiotic detoxification, they may also act as peroxidases or regenerating ascorbate (Dixon et al., 2009). Increases in expression of *GSTs* in response to exogenous ethylene were less relevant and declined after transferring the fruits to air (Supplementary Table S3). This indicates that the stress caused by ethylene may be reversible. *GSTs* may thus participate in the cross-protection responses induced by the hormone and may also be induced in the 1-MCP-treated fruits to cope with the persistence of ROS or xenobiotics caused by an excess of ethylene and/or its co-products. In this regard, previous data showed the involvement of ROS in ethylene-induced damage in plants (Hodges and Forney, 2000). The fact that 1-MCP barely affected the alternative respiration and the UCP pathways (Fig. 4) is remarkable since it indicates that they would not contribute to ROS prevention in 1-MCP-treated fruits. Likewise, changes in the ethylene-treated oranges agree with the idea that the ethylene-induced acclimation of plants to stress involves oxidative stress-related responses (Munné-Bosch et al., 2004). An excess of ethylene may favor ROS and senescence (Hodges and Forney, 2000) and some of the 1-MCP-induced responses showed similarities to the responses related to the postharvest senescence process in citrus fruit (Ding et al., 2015). However, besides NCPP incidence, there were no relevant differences in external appearance among AC, EC and 1-MCP-treated fruits. Therefore, senescence appears not to be a limiting factor for NCPP development.

The activation of *GSTs* and other stress-related responses further suggests that an excess of cyanide and NO may contribute to the 1-MCP-induced damage. It was surprising to find the over-representation of processes related to defense response to pathogens since these processes were not up-regulated by ethylene in the present work or in infected citrus fruit (Gonzalez-Candelas et al., 2010). Cyanide and NO stimulate responses associated with the plant immune system (García et al., 2013; Scheler et al., 2013). Therefore, these compounds might modulate additional responses to those regulated by the hormone in the 1-MCP-treated fruits. It is worth noticing that both

cyanide and 1-MCP trigger similar oxidative stress-related responses, such as the induction of genes encoding amine oxidases or involved in signalling within the MAPK and Ser/ThrPK cascade, as well as the repression of *CAT* and *Cu/Zn SODs* (Oracz et al., 2009). Considering these results, and that cyanide increases the expression of hypoxic responsive genes, as 1-MCP does, the participation of cyanide in the development of peel damage was confirmed by showing that SNP mimicked the NCPP syndrome and that HB reduced it in the 1-MCP-treated fruit. What we may learn from these results is that some of the 1-MCP-related responses may be associated with cyanide. This finding might help to understand the different effects of 1-MCP on damage in different fruits. Cyanide release might explain in part why 1-MCP favors stress-induced disorders in citrus fruits but reduces them in apple fruit. Contrary to what happens in citrus fruit, apples shows high and autocatalytic ethylene production, 1-MCP reduces ethylene biosynthesis in apples, and hence cyanide levels must be lower in MCP-treated apples. Another example of the relevance of this finding is the suggestion that cyanide might influence the response of antisense ACO plants and fruits to stresses, since ethylene, but also cyanide formation, should be curtailed in these plants.

The link between ethylene/cyanide and NO release remains unknown, although it has been reported that some effects of cyanide can be mediated through NO (Bethke et al., 2006). Results from the present study showed that 1-MCP induced the response to salicylic acid stimulus in citrus fruit and has the thylakoid membrane and the Calvin cycle as target sites (Table 2 and Fig. 4), which resembles cyanide- and NO-related changes in plants (García et al., 2013; Scheler et al., 2013). 1-MCP induced other NO stress-related responses (Parani et al., 2004) and specifically over-expressed the PCD, **the ‘defense response, immune interaction’ and the ‘jasmonic acid mediated signalling pathway’ biological processes in mature oranges (Table 1)**. In the context of the present work, it is noticing that NO and ROS signalling pathways are connected and related to cell death (Van Breusegem and Dat, 2006; Wodala, 2006) and to plant defense mechanisms involving plant biotic interactions (Scheler et al., 2013). Likewise, the ethylene and the 1-MCP-induced changes in abundant LOX-encoding genes (Supplementary Table S2) within the oxylipin metabolic process found in the present work resembled results showing that prolonged NO stress inhibit LOX isoforms in spite of LOX activity increases at the beginning of NO stress (Arasimowicz and Floryszak-Wieczorek, 2007). Considering these findings, the participation of NO in the harmful effect of 1-MCP was further confirmed by applying SNP as well as cPTIO. The facts

that HB and cPTIO were very effective in reducing 1-MCP-enhanced damage further indicated a higher influence of an excess of ethylene and/or its co-products than the higher energy requirements of the detached 1-MCP-treated citrus fruits on NCCP development.

585 In conclusion, 1-MCP mimics, at long-term, stress-related responses and triggers the overproduction of ethylene and metabolic shifts aimed to cope with cell toxicity and increased respiration and extra energy demand in detached non-climacteric citrus fruit. Although the external manifestation of NCCP affects the flavedo, global data indicate that the albedo is the most affected tissue in this disorder. Cyanide and NO may
590 converge in the toxic effects of 1-MCP. ROS and/or xenobiotic downstream mechanisms might act as signals for defense responses in the EC fruit, while a higher uncontrolled generation of ethylene/cyanide in the 1-MCP-treated fruits would lead to damage. Another lesson to be learned from this work is that further attention should be paid to understanding the effects of ethylene co-products on the physiological effects
595 attributed until now only to the hormone. Such effects may vary the interpretation of results derived from 1-MCP application when studying the role of ethylene, associated with sharp increases/decreases in endogenous ethylene levels, or derived from transgenic fruit and plants with altered ethylene biosynthesis.

600

SUPPLEMENTARY MATERIAL

Supplemental Fig. S1. NCPP syndrome in fruit held in air (A), and in fruits pretreated with 1-MCP (B) and SNP (C).

605 Supplemental Fig. S2. Correlation in the expression of selected genes (Table S1) quantified using either the citrus microarray or RT-qPCR. The expression of these genes was quantified in the flavedo and albedo of AC, EC and 1-MCP fruits stored for 4 and 14 days at 20 °C ($r^2 = 0.807$, $p \leq 0.05$).

610 Supplemental Fig. S3. Effect of **HB (■)** and **cPTIO (▲)** on the **ethylene production** of fruits treated with 1-MCP (●) and stored at 20 °C. No significant differences were found among mean values of these samples for the same storage period ($p \leq 0.05$), and the **values always differed significantly from the means of fruits treated only with water (○)**.

615 Supplemental Table S1. Selected genes and primers used for comparison between the *Citrus* 12 k microarray and RT-qPCR gene expression data. Reference genes *CsACT*, *CsEF1 α* , and *CsTUB* were used for data normalization.

Supplemental Table S2. Expression levels of citrus genes in the flavedo (F) and albedo (A) of AC, EC and 1-MCP-treated fruit stored for 4 and 14 days at 20 °C grouped according to the biological processes they belong to. Numbers in bold indicate statistically significant differences (SAM, FDR < 0.01).

620

Supplemental Table S3. Fold changes (\log_2) in expression of oxidative stress-related genes in the flavedo (F) and albedo (A) of AC, EC and 1-MCP-treated fruits stored for 4 and 14 days at 20 °C as compared to freshly harvested (FH) fruit. The symbol + indicates no expression in FH fruits, and the symbol – indicates expression in FH fruits but not in the compared treatment. Numbers in bold indicate differential expression in the compared condition according to SAM (FDR < 0.01).

625

630

5. ACKNOWLEDGEMENTS

Special thanks to Dr. J. Gadea and Dr. J. Forment (CFGP) for their help in microarray generation and for bioinformatics assistance. This work was supported by
635 the Spanish Ministry of Science and Technology (Research Grants AGL2002-1727 and
AGL2009-11969 and by the Generalitat Valenciana, Spain (Grant PROMETEOII/2014/027). Dr. B. E. was the recipient of a fellowship of the Spanish
Ministry of Science and Technology. Dr. A.R.B. is grateful to CSIC and the European
Social Fund for her postdoctoral JAE-Doc contract.

640

6. CONTRIBUTIONS

LGC, BE and MTL designed the research. BE and MTL performed the treatments
645 and BE the microarray experiments. LGC, AB and PR contributed to the bioinformatics
analyses. AB and PR designed primers used for the transcription studies and performed
the expression assays. MTL performed experiments related to fruit physiology and LGC
and MTL wrote the paper. All the authors contributed to improve the paper and
approved the final manuscript.

650

7. REFERENCES

- 655 Abeles, F.B., Morgan, P.W., Satlveit, M.E.J., 1992. Ethylene in plant biology, second ed. Academic Press, San Diego, CA.
- Arasimowicz, M., Floryszak-Wieczorek, J., 2007. Nitric oxide as a bioactive signalling molecule in plant stress responses. *Plant Sci.* 172, 876–887.
- Asada, K., 2006. Production and scavenging of reactive oxygen species in chloroplasts and their functions. *Plant Physiol.* 141, 391–396.
- 660 Bailey-Serres, J., Fukao, T., Gibbs, D.J., Holdsworth, M.J., Lee, S.C., Licausi, F., Perata, P., Voesenek, L.A.C.J., van Dongen, J.T., 2012. Making sense of low oxygen sensing. *Trends Plant Sci.* 17, 129–138.
- Ballester, A.R., Lafuente, M.T., Forment, J., Gadea, J., De Vos, C.H.R., Bovy, A.G., González-Candelas, L., 2011. Transcriptomic profiling of citrus fruit peel tissues reveals fundamental effects of phenylpropanoids and ethylene on induced resistance. *Mol. Plant Pathol.* 12, 879–897.
- 665 Bethke, P.C., Libourel, I.G.L., Reinöhl, V., Jones, R.L., 2006. Sodium nitroprusside, cyanide, nitrite, and nitrate break *Arabidopsis* seed dormancy in a nitric oxide-dependent manner. *Planta* 223, 805–812.
- 670 Cajuste, J.F., García-Breijo, F.J., Reig-Armiñana, J., Lafuente, M.T., 2011. Ultrastructural and histochemical analysis reveals ethylene-induced responses underlying reduced peel collapse in detached citrus fruit. *Microsc. Res. Tech.* 74, 970–979.
- 675 Cools, K., Chope, G.A., Hammond, J.P., Thompson, A.J., Terry, L.A., 2011. Ethylene and 1-methylcyclopropene differentially regulate gene expression during onion sprout suppression. *Plant Physiol.* 156, 1639–1652.
- Ding, Y., Chang, J., Ma, Q., Chen, L., Liu, S., Jin, S., Han, J., Xu, R., Zhu, A., Guo, J., Luo, Y., Xu, J., Xu, Q., Zeng, Y., Deng, X., Cheng, Y., 2015. Network analysis of postharvest senescence process in citrus fruits revealed by transcriptomic and metabolomic profiling. *Plant Physiol.* 168, 357–376.
- 680 Dixon, D.P., Hawkins, T., Hussey, P.J., Edwards, R., 2009. Enzyme activities and subcellular localization of members of the *Arabidopsis* glutathione transferase superfamily. *J. Exp. Bot.* 60, 1207–1218.
- 685 Fujii, H., Shimada, T., Sugiyama, A., Nishikawa, F., Endo, T., Nakano, M., Ikoma, Y., Shimizu, T., Omura, M., 2007. Profiling ethylene-responsive genes in mature mandarin fruit using a citrus 22K oligoarray. *Plant Sci.* 173, 340–348.
- García, I., Rosas, T., Bejarano, E.R., Gotor, C., Romero, L.C., 2013. Transient transcriptional regulation of the *CYS-C1* gene and cyanide accumulation upon pathogen infection in the plant immune response. *Plant Physiol.* 162, 2015–2027.
- 690 Gonzalez-Candelas, L., Alamar, S., Sanchez-Torres, P., Zacarias, L., Marcos, J., 2010. A transcriptomic approach highlights induction of secondary metabolism in citrus fruit in response to *Penicillium digitatum* infection. *BMC Plant Biol.* 10, 194–211.
- Hodges, D.M., Forney, C.F., 2000. The effects of ethylene, depressed oxygen and elevated carbon dioxide on antioxidant profiles of senescing spinach leaves. *J. Exp. Bot.* 51, 645–655.
- 695 Huber, D.J., Hurr, B.M., Lee, J.S., Lee, J.H., 2010. 1-Methylcyclopropene sorption by tissues and cell-free extracts from fruits and vegetables: Evidence for enzymic 1-MCP metabolism. *Postharvest Biol. Technol.* 56, 123–130.
- 700 John-Karuppiah, K.-J., Burns, J.K., 2010. Degreening behavior in ‘Fallglo’ and ‘Lee x Orlando’ is correlated with differential expression of ethylene signaling and biosynthesis genes. *Postharvest Biol. Technol.* 58, 185–193.

- Lafuente, M.T., Sala, J.M., 2002. Abscisic acid levels and the influence of ethylene, humidity and storage temperature on the incidence of postharvest rindstaining of 'Navelina' orange (*Citrus sinensis* L. Osbeck) fruit. *Postharvest Biol. Technol.* 25, 49–57.
- 705 Lafuente, M.T., Zacarías, L., Martínez-Téllez, M.A., Sánchez-Ballesta, M.T., Dupille, E., 2001. Phenylalanine ammonia-lyase as related to ethylene in the development of chilling symptoms during cold storage of citrus fruits. *J. Agric. Food Chem.* 49, 6020–6025.
- 710 Marcos, J.F., González-Candelas, L., Zacarías, L., 2005. Involvement of ethylene biosynthesis and perception in the susceptibility of citrus fruit to *Penicillium digitatum* infection and the accumulation of defense-related mRNAs. *J. Exp. Bot.* 56, 2183–2193.
- 715 Martínez-Godoy, A.M., Mauri, N., Juárez, J., Marques, C.M., Santiago, J., Forment, J., Gadea, J., 2008. A genome-wide 20 K citrus microarray for gene expression analysis. *BMC Genomics* 9 318–329.
- 720 Matas, A.J., Yeats, T.H., Buda, G.J., Zheng, Y., Chatterjee, S., Tohge, T., Ponnala, L., Adato, A., Aharoni, A., Stark, R., Fernie, A.R., Fei, Z., Giovannoni, J.J., Rose, J.K.C., 2011. Tissue- and cell-type specific transcriptome profiling of expanding tomato fruit provides insights into metabolic and regulatory specialization and cuticle formation. *Plant Cell* 23, 3893–3910.
- McCollum, G., Maul, P., 2007. 1-Methylcyclopropene inhibits degreening but stimulates respiration and ethylene biosynthesis in grapefruit. *Hortsci.* 42, 120–124.
- 725 Munné-Bosch, S., Peñuelas, J., Asensio, D., Llusà, J., 2004. Airborne ethylene may alter antioxidant protection and reduce tolerance of holm oak to heat and drought stress. *Plant Physiol.* 136, 2937–2947.
- Oracz, K., El-Maarouf-Bouteau, H., Kranner, I., Bogatek, R., Corbineau, F., Bailly, C., 2009. The mechanisms involved in seed dormancy alleviation by hydrogen cyanide unravel the role of reactive oxygen species as key factors of cellular signaling during germination. *Plant Physiol.* 150, 494–505.
- 730 Parani, M., Rudrabhatla, S., Myers, R., Weirich, H., Smith, B., Leaman, D.W., Goldman, S.L., 2004. Microarray analysis of nitric oxide responsive transcripts in *Arabidopsis*. *Plant Biotechnol. J.* 2, 359–366.
- 735 Peiser, G.D., Wang, T.-T., Hoffman, N.E., Yang, S.F., Liu, H.-w., Walsh, C.T., 1984. Formation of cyanide from carbon 1 of 1-aminocyclopropane-1-carboxylic acid during its conversion to ethylene. *Proc. Natl. Acad. Sci. U. S. A.* 81, 3059–3063.
- Prange, R., Daniels-Lake, B., Jeong, J.-C., Binns, M., 2005. Effects of ethylene and 1-methylcyclopropene on potato tuber sprout control and fry color. *Am. J. Potato Res.* 82, 123–128.
- 740 Purvis, A.C., 1980. Sequence of chloroplast degreening in calamondin fruit as influenced by ethylene and AgNO₃. *Plant Physiol.* 66, 624–627.
- Riechers, D.E., Kreuz, K., Zhang, Q., 2010. Detoxification without intoxication: Herbicide safeners activate plant defense gene expression. *Plant Physiol.* 153, 3–13.
- 745 Romero, P., Rodrigo, M.J., Alferez, F., Ballester, A.R., González-Candelas, L., Zacarías, L., Lafuente, M.T., 2012. Unravelling molecular responses to moderate dehydration in sweet orange (*Citrus sinensis* L. Osbeck) by using a fruit-specific ABA-deficient mutant. *J. Exp. Bot.* 63, 2753–2767
- 750 Scheler, C., Durner, J., Astier, J., 2013. Nitric oxide and reactive oxygen species in plant biotic interactions. *Curr. Opin. Plant Biol.* 16, 534–539.

- Theologis, A., Laties, G.G., 1981. Wound-induced membrane lipid breakdown in potato tuber. *Plant Physiol.* 68, 53-58.
- 755 Thimm, O., Bläsing, O., Gibon, Y., Nagel, A., Meyer, S., Krüger, P., Selbig, J., Müller, L.A., Rhee, S.Y., Stitt, M., 2004. MAPMAN: a user-driven tool to display genomics data sets onto diagrams of metabolic pathways and other biological processes. *Plant J.* 37, 914-939.
- Van Breusegem, F., Dat, J., 2006. Reactive oxygen species in plant cell death. *Plant Physiol.* 141, 384-390.
- 760 Wang, P., Zhang, B., Li, X., Xu, C., Yin, X., Shan, L., Ferguson, I., Chen, K., 2010. Ethylene signal transduction elements involved in chilling injury in non-climacteric loquat fruit. *J. Exp. Bot.* 61, 179-190.
- Watkins, C.B., 2006. The use of 1-methylcyclopropene (1-MCP) on fruits and vegetables. *Biotechnol. Adv.* 24, 389-409.
- 765 Wodala, B., 2006. Combined effects of nitric oxide and cyanide on the photosynthetic electron transport of intact leaves. *Acta Biologica Szegediensis* 50 (3-4), 185.
- Zabalza, A., Van Dongen, J.T., Froehlich, A., Oliver, S.N., Faix, B., Gupta, K.J., Schmäzlin, E., Igal, M., Orcaray, L., Royuela, M., Geigenberger, P., 2009. Regulation of respiration and fermentation to control the plant internal oxygen concentration. *Plant Physiol.* 149, 1087-1098.
- 770

Figure Legends

Figure 1. Schematic diagram of the experimental design.

775 Figure 2. Ethylene (A), CO₂ production (B) and non-chilling peel pitting (NCPPI) index (C) of 'Navelate' fruits stored at 20 °C. Fruits were held in i) air (○, AC control); ii) air after being conditioned for 4 days with 10 μL L⁻¹ ethylene (□, EC); and iii) air after being treated for 14 h with 1 μL L⁻¹ 1-MCP (■, 1-MCP). Insert panel in Fig. 2A shows values corresponding to the ethylene production of the control AC fruits and of the EC fruits on a smaller scale to better illustrate differences found in these samples. Significant differences ($p \leq 0.05$) within the same storage period in CO₂ production between AC and EC or 1-MCP-treated fruits are labelled with one or two asterisks, respectively. Significant differences in ethylene production and in NCPPI index between 1-MCP-treated samples and AC samples were found from day 4. 780 NCPPI index in EC fruits was lower than in AC and 1-MCP-treated fruits from day 3. Significant differences in ethylene production between AC and EC samples are labelled with an asterisk in the insert panel. Error bars represent SE.

Figure 3. Venn diagrams showing the number of differentially expressed genes (SAM, FDR<0.01) in the flavedo (A, B) and albedo (C,D) of AC (control), EC and 1-MCP-treated 'Navelate' fruits stored for 4 (A,C) and 14 days (B,D) at 20 °C. Expression levels of up-regulated (bold) and down-regulated (italics) genes in these samples were compared with the levels of freshly harvested fruits. Numbers in brackets are the sum of all induced and repressed genes under each particular condition. The sizes of the circles are shown relative to the total number of differentially expressed genes for each condition. 795

Figure 4. Metabolic overview using MapMan (Thimm et al., 2004) comparing transcript accumulation in the albedo of 1-MCP-treated (A) and of control air (AC) (B) fruits held for 14 days at 20 °C. Red and blue squares represent transcripts with decreasing and increasing levels, respectively, with respect to freshly harvested fruit. Color scale is indicated in the figure. 800

Figure 5. Effect of increasing concentrations of SNP (A) and of 300 μM HB (■) and 300 μM cPTIO (▲) on NCPPI index of fruits treated with 1 μL L⁻¹ 1-MCP (●) and stored at 20 °C in air (B). Results are represented as means of the three replicate samples. Significant differences ($P \leq 0.05$) in NCPPI index between fruits treated with different SNP concentrations (A) are indicated by different letters. Means 805

within Fig. 5B labelled with the same letter for the same storage period did not differ significantly ($p \leq 0.05$). Significant differences in peel damage index were not found between air and HB+1-MCP-treated fruits within the same storage period.

Table 1. Gene ontology (GO) analysis (FatiGO+, $P < 0.05$) of biological processes over- (↑) or infra-represented (↓) in the flavedo (F) or albedo (A) of air (AC control fruits), EC (ethylene) and 1-MCP-treated fruits (1-MCP), with respect to freshly harvested fruit. Black bars refer to the 815 treatments in which the processes included in a specific pattern were differentially expressed. Lower GO levels represent general biological processes, whereas higher levels denote more precise information.

GO Level	GO Code	Description	Pattern of expression										
			4 days			14 days							
			Air		Ethylene		1-MCP		Air		Ethylene		1-MCP
F	A	F	A	F	A	F	A	F	A	F	A		
820	Pattern 1	Differentially expressed only by 1-MCP											
	3	0007154											↑
	3	0008037											↑
	3	0006955											↑
	4	0006793											↑
	4	0006970											↑
	4	0009636											↑
	4	0006952											↑
	5	0006796											↑
825	5	0010038											↑
	5	0009651											↑
	5	0007165											↑
	5	0045087											↑
	5	0012501											↑
	5	0009620											↑
	5	0009751											↑
	6	0016310											↑
	6	0009723											↑
	6	0006464											↑
	6	0009814											↑
	7	0043687											↑
	7	0006468											↑
	8	0009867											↑
830	Pattern 2	Differentially expressed by Air and/or Ethylene but not by 1-MCP											
	4	0006629	↑		↑								
	4	0015977	↓	↓	↓								
	5	0008610	↑		↑	↑							
	8	0006631							↑				
	9	0006633							↑				
835	Pattern 3	Differentially expressed by Ethylene and 1-MCP											
	3	0042221			↑	↑							↑
	3	0006950			↑	↑							↑
	5	0009743				↑							↑
	6	0046686			↑								↑
	6	0010200				↑							↑
	7	0009813			↑	↑							↑
	9	0042398			↑	↑							↑
840	Pattern 4	Differentially expressed by Ethylene but not by Air or 1-MCP											
	3	0009628			↓	↓							
	3	0019748			↑	↑							
	3	0009605			↑								
	4	0015979			↓	↓							
	4	0006790			↑	↑							
	4	0009314			↓								
	4	0008104				↑							
	5	0009698			↑	↑							
	5	0009416			↓								
	5	0019684				↓							
	5	0001666				↓							
	5	0009409				↓							
	6	0009808			↑	↑							
	6	0009699			↑	↑							
	6	0015031				↑							
	7	0009809			↑	↑							
	9	0031407			↑								↑
845	Pattern 5	Differentially expressed by Air or 1-MCP but not by Ethylene											
	3	0009607	↑	↓									↑
	4	0010033	↑										↑
	4	0051707		↓									↑
	6	0009753	↑										↑
845	Pattern 6	Differentially expressed by Air but not by 1-MCP or Ethylene											
	5	0016051											↓
	6	0009966	↑										
	7	0009968	↑										
	8	0009072	↑										
	9	0009073	↑										

Table 2. Gene ontology (GO) analysis (FatiGO+, $P < 0.05$) of molecular function, cellular component and interpro domain over-(\uparrow) or infra-represented (\downarrow) in the flavedo (F) or albedo (A) tissues of 'Navelate' oranges held in air (AC, control), conditioned for 4 days with ethylene and transferred to air (EC), or treated with 1-MCP and held in air (MCP), with respect to freshly harvested fruit.

GO Level	GO Code	Description	Pattern of expression											
			4 days			14 days								
			AC	EC	MCP	AC	EC	MCP						
			F	A	F	A	F	A	F	A				
Molecular function														
5	0016773	phosphotransferase activity, alcohol group as									\uparrow	\uparrow		
5	0046982	protein heterodimerization activity									\uparrow			
6	0004672	protein kinase activity									\uparrow	\uparrow		
6	0046914	transition metal ion binding									\uparrow			
7	0004674	protein serine/threonine kinase activity									\uparrow	\uparrow		
7	0004713	protein tyrosine kinase activity									\uparrow	\uparrow		
8	0017076	purine nucleotide binding										\uparrow		
9	0005524	ATP binding										\uparrow		
5	0016301	kinase activity										\uparrow	\uparrow	
8	0020037	heme binding										\uparrow		
9	0005506	iron ion binding										\uparrow	\uparrow	
5	0008194	UDP-glycosyltransferase activity												
5	0016705	oxidoreductase activity, acting on paired donors, with incorporation or reduction of molecular oxygen												
5	0016616	oxidoreductase activity, acting on the CH-OH group of donors, NAD or NADP as acceptor												
5	0016757	transferase activity, transferring glycosyl groups												
5	0016702	oxidoreductase activity, acting on single donors with incorporation of molecular oxygen, incorporation of											\uparrow	
6	0019205	nucleobase, nucleoside, nucleotide kinase activity												
6	0016776	phosphotransferase activity, phosphate group as acceptor												
7	0019201	nucleotide kinase activity												
5	0004497	monooxygenase activity											\uparrow	
Cellular Component														
5	0005886	plasma membrane											\uparrow	
6	0009579	thylakoid											\downarrow	
9	0042651	thylakoid membrane											\downarrow	
5	0009523	photosystem II											\downarrow	
9	0009521	photosystem											\downarrow	
InterPro														
	IPR017442	Serine/threonine protein kinase-related											\uparrow	\uparrow
	IPR008271	Serine/threonine protein kinase, active site											\uparrow	\uparrow
	IPR017441	Protein kinase, ATP binding site											\uparrow	\uparrow
	IPR001246	Lipoxygenase, plant											\uparrow	\uparrow
	IPR013819	Lipoxygenase, C-terminal											\uparrow	\uparrow
	IPR016040	NAD(P)-binding domain											\uparrow	
	IPR008976	Lipase/lipoxygenase, PLAT/LH2											\uparrow	
	IPR001024	Lipoxygenase, LH2											\uparrow	
	IPR013747	3-Oxoacyl-[acyl-carrier-protein (ACP)] synthase III											\uparrow	
	IPR012328	Chalcone/stilbene synthase, C-terminal											\uparrow	
	IPR013601	FAE1/Type III polyketide synthase-like protein											\uparrow	
	IPR016039	Thiolase-like											\uparrow	
	IPR012392	Very-long-chain 3-ketoacyl-CoA synthase											\uparrow	

855 Table 3. Relative expression level of genes involved in ethylene biosynthesis, perception and
 860 signalling, and in cyanide detoxification, printed in the microarray and differentially expressed
 in the albedo (A) and/or flavedo (F) of AC (air, control), EC and 1-MCP-treated ‘Navelate’
 fruits. The symbol + indicates no expression in freshly harvested fruits, and the symbol –
 indicates expression in freshly harvested fruits but not in the compared treatment. Numbers in
 bold indicate differential expression in the compared condition according to SAM ($P < 0.01$)

Citrus unigene	Description	4 days						14 days					
		AC		EC		1-MCP		AC		EC		1-MCP	
		F	A	F	A	F	A	F	A	F	A	F	A
Fold Change (\log_2)													
<i>Ethylene biosynthesis</i>													
aCL414Contig2	S-adenosyl-L-methionine synthetase 1	0.08	0.16	0.36	0.68	-0.16	0.06	-0.14	-0.05	-0.35	0.00	0.87	0.55
aC08030G11SK_c	S-adenosylmethionine synthetase	0.28	+	0.60		-	+	-0.11	+	0.03	+	-0.02	+
aC31207B09EF_c	S-adenosylmethionine synthetase	0.34	0.15	0.50	0.52	-0.18	-0.04	0.08	-0.19	-0.15	-0.12	0.44	0.27
aCL33Contig2	S-adenosylmethionine synthetase 2	0.24	0.19	0.52	0.12	-0.13	-0.06	0.05	-	0.03	-	-	-0.02
865 aCL55Contig2	S-adenosylmethionine synthetase 2	0.45	0.27	0.82	0.81	-0.80	-0.77	-0.23	-0.81	-0.37	-0.34	1.26	0.59
aCL7172Contig1	ACC synthase	-0.18	0.21	0.42	1.07	0.33	0.95	-0.36	0.40	-0.22	0.23	-	2.01
aCL4017Contig1	ACC synthase	-0.13	-0.06	0.03	-0.02	-0.05	0.14	-0.11	0.01	-0.17	-0.13	-0.20	0.60
aC31605B08EF_c	ACC oxidase	-0.22	0.24	0.48	1.73	1.25	2.08	-0.91	-0.25	-1.84	-0.22	1.27	3.96
aCL4439Contig1	ACC oxidase 1	1.43	0.23	2.04	1.21	2.64	2.07	0.70	0.45	-0.32	0.19	2.45	2.89
aCL3488Contig1	ACC oxidase ACCO2	-0.40	-0.10	-0.12	0.36	0.53	0.00	-0.10	-0.05	0.18	0.36	0.35	1.40
aCL7299Contig1	Ethylene-forming-enzyme-like dioxygenase	0.07	0.33	0.48	0.66	2.73	0.58	0.13	0.36	0.03	0.26	0.06	0.89
aC08019A01SK_c	Ethylene-forming-enzyme-like dioxygenase	-0.17	0.33	0.37	0.49	0.45	0.61	-0.30	0.11	-0.44	-0.03	-0.03	0.68
aC31703B04EF_c	Putative ethylene-forming enzyme	-0.10	0.74	0.03	0.70	-0.52	0.03	-0.09	0.43	-0.19	0.24	-0.09	0.04
<i>Ethylene perception/signaling</i>													
aCL3291Contig1	Ethylene receptor	0.29	0.33	0.05	0.13	-0.19	-0.54	-0.23	-0.46	-0.32	-0.51	0.27	-0.10
870 aCL7399Contig1	Ethylene receptor homolog	-0.09	0.75	-0.29	0.01	-0.09	-0.34	-0.07	0.01	-0.27	0.21	1.09	0.56
aCL7700Contig1	Putative ethylene receptor	0.73	1.62	0.40	0.99	0.85	0.45	0.55	0.31	0.51	0.59	1.49	1.72
aCL5522Contig1	Anther ethylene-upregulated protein ER1	0.36	0.08	0.05	0.02	0.37	0.09	0.38	-0.06	0.51	0.08	0.62	0.46
aCL5870Contig1	Auxin and ethylene responsive GH3-like prot	0.98	1.24	0.93	1.78	0.09	-0.33	0.23	-0.04	-0.08	0.03	0.66	0.05
aCL7060Contig1	AP2/EREBP transcription factor ERF-2	0.17	0.72	-0.27	0.14	0.09	0.34	0.27	0.64	0.33	0.72	0.48	0.27
aCL1363Contig1	AP2/EREBP transcription factor ERF-2	0.23	0.60	0.04	-0.01	0.36	0.15	0.41	0.34	0.38	0.56	0.69	0.26
aCL1567Contig2	Putative ethylene response factor ERF3a	0.36	0.29	-0.14	0.48	0.24	0.47	0.03	0.88	-0.19	0.88	0.56	0.86
aCL337Contig1	Putative ethylene response factor 5	0.24	-0.04	0.31	0.77	1.04	1.02	-0.16	0.85	0.01	0.63	0.60	0.55
aCL5870Contig1	Auxin and ethylene responsive GH3-like prot	0.98	1.24	0.93	1.78	0.09	-0.33	0.23	-0.04	-0.08	0.03	0.66	0.05
aCL9142Contig1	Ethylene-responsive element binding factor	-0.10	0.03	-0.33	0.08	0.64	0.02	0.63	0.46	0.01	0.14	-0.09	-0.59
875 aCL152Contig1	Ethylene-responsive factor-like protein 1	0.31	0.18	0.85	0.86	0.57	0.30	0.57	1.06	0.80	1.28	1.04	1.21
aCL2320Contig1	Ethylene-responsive transcription factor 13	-0.68	-0.56	-0.99	-0.92	-0.78	-0.79	-0.36	-0.73	-0.31	-0.73	-1.06	-1.19
aCL1087Contig1	Ethylene responsive element binding prot	-0.02	0.37	-0.07	0.33	1.03	1.08	0.49	0.84	-0.20	0.42	0.69	0.94
aCL5023Contig1	EIN3-like protein	0.32	0.67	-0.16	0.40	0.39	0.20	0.44	0.36	0.32	0.66	0.99	0.36
<i>Cyanide detoxification</i>													
aC06021C12SK_c	Beta-cyanoalanine synthase	0.17	0.22	-0.05	0.40	-0.04	-0.04	-0.13	-0.02	-0.03	-0.09	-0.05	-0.01
aCL5505Contig1	Beta-cyanoalanine synthase	1.66	4.23	2.18	4.51	-1.91	-1.49	-0.95	0.89	-1.96	0.66	2.18	2.92
aC31502A08EF_c	Nitrilase 4	0.68	1.12	0.45	1.17	0.29	0.38	0.42	0.73	0.38	0.79	1.17	1.21
aCL6373Contig1	Putative alpha-hydroxynitrile lyase	0.10	-0.05	-0.31	-0.41	0.33	0.10	0.25	-0.03	0.33	0.01	-0.45	-0.17
aCL4704Contig1	Putative alpha-hydroxynitrile lyase	0.31	0.43	0.51	0.92	0.44	0.13	-0.08	0.03	0.17	0.12	1.08	1.31

880

885 Table 4. Classification of xenobiotic/cyanide-related genes up- (U) and down- (D) regulated in the flavedo and/or albedo of 'Navelate' fruits held in air (AC, control), treated for 4 days with ethylene and then transferred to air (EC) or treated with 1-MCP before holding in air (MCP), with respect to freshly harvested fruit. Blanks indicate that no gene was either up- or down-regulated in the compared treatment

Description	Probes ^a	Flavedo						Albedo					
		4 days			14 days			4 days			14 days		
		AC	EC	MCP	AC	EC	MCP	AC	EC	MCP	AC	EC	MCP
		U/D	U/D	U/D	U/D	U/D	U/D	U/D	U/D	U/D	U/D	U/D	U/D
890 <i>Glutathione S-transferase</i>	27	1/0	7/0			10/0	3/0	7/1	3/0	2/0	2/0	17/1	
<i>Cytochrome P450</i>	50	1/1	4/3		0/1	1/0	5/1	6/2	13/2	1/0	3/1	3/1	21/3
<i>Gycosyl/glucosyltransferase</i>	62	1/1	11/0		2/0	1/2	3/3	1/2	11/1	0/2	0/2	0/2	14/4
<i>O-methyltransferase</i>	29		5/1		0/1		4/1	1/1	4/1		0/1	0/1	13/3
<i>Peptidases</i>	66		1/0		0/2	0/1	1/0	4/0	5/0	3/0	3/0	7/0	18/2
<i>Calcium/calmodulin-binding</i>	20	0/1	2/2		2/2		2/2	1/2	5/3	2/1	1/3	1/2	11/6
895 <i>ABC transporters</i>	32	1/1	3/2	0/2	4/2	3/1	3/1	2/0	5/1	2/1	3/0		11/2

^aTotal number of probes in the microarray

CONTRIBUTIONS: LGC, BE and MTL designed the research. BE and MTL performed the treatments and BE the microarray experiments. LGC, AB and PR contributed to the bioinformatics analyses. AB and PR designed primers used for the transcription studies and performed the expression assays. MTL performed experiments related to fruit physiology and LGC and MTL wrote the paper. All the authors contributed to improve the paper and approved the final manuscript.

Revised Fig. 1

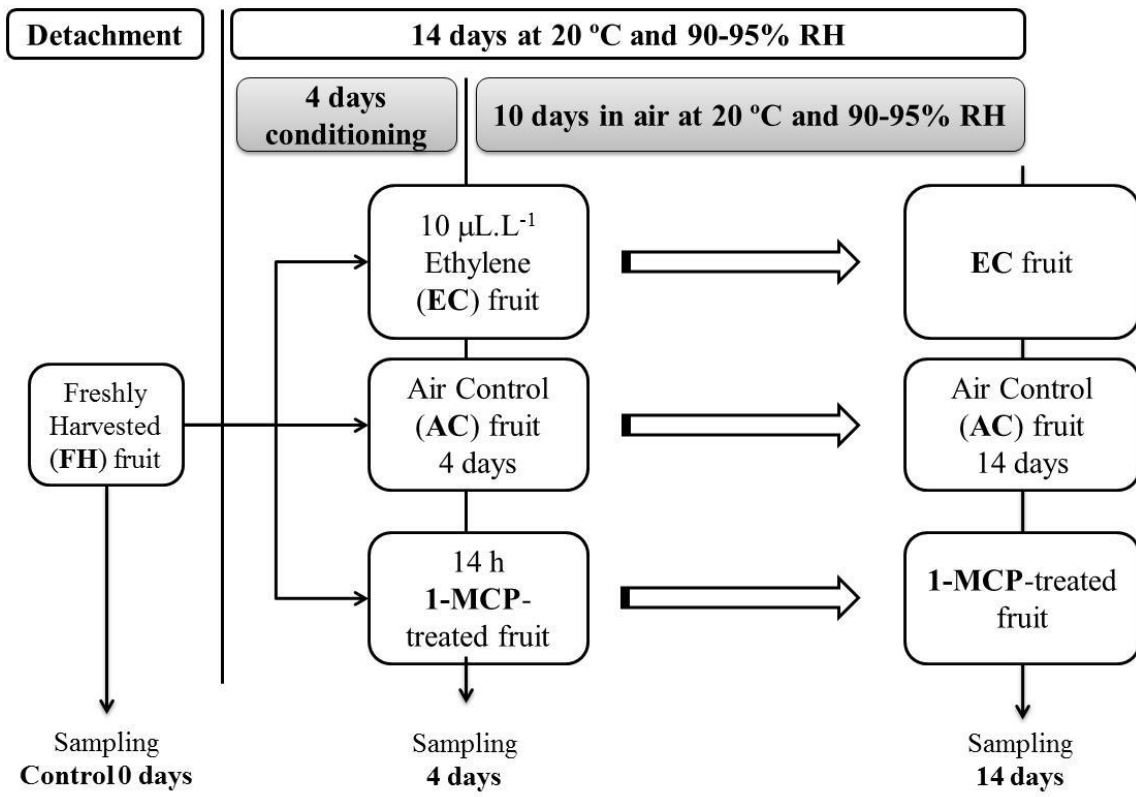


Fig. 2

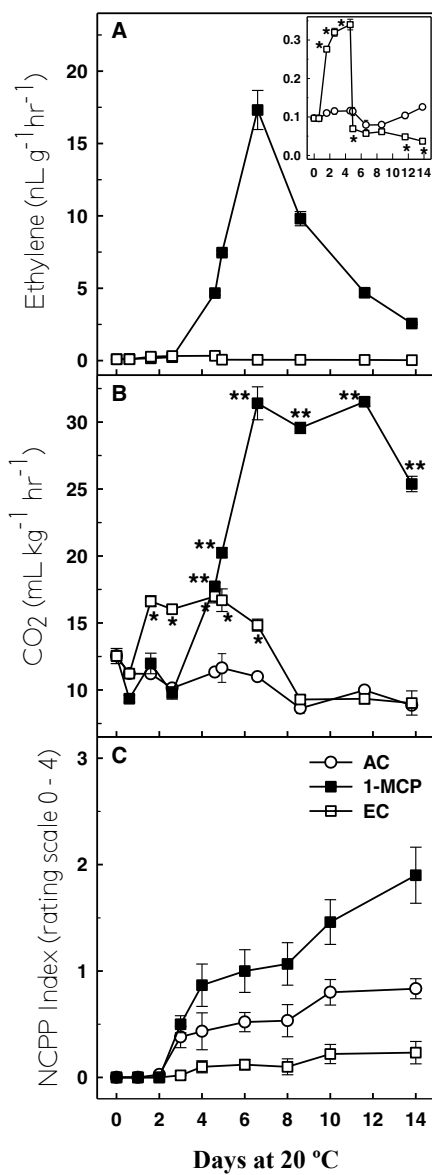


Figure 3

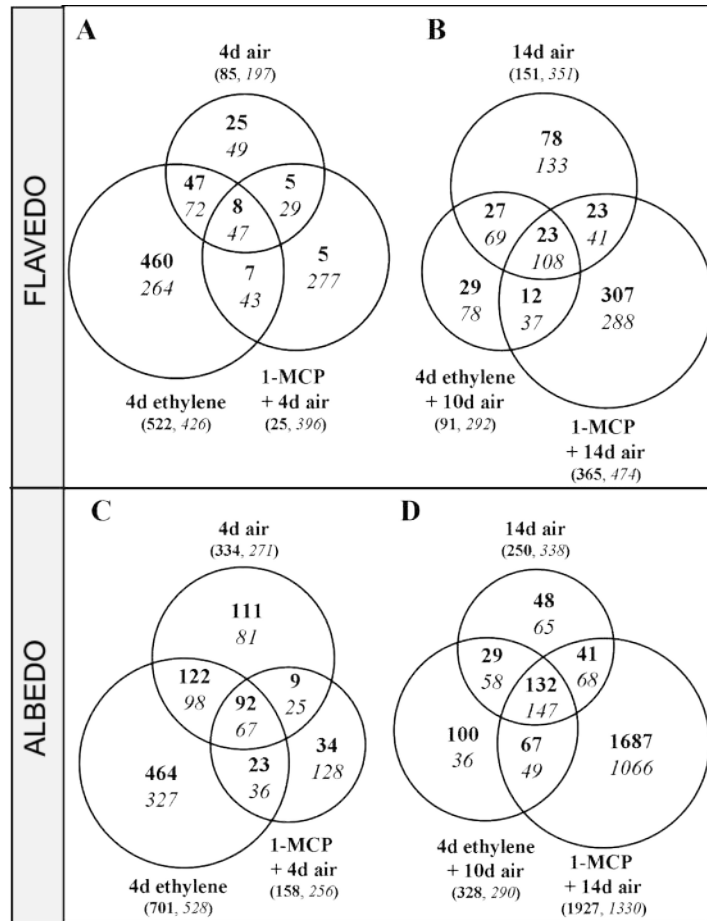


Figure 3

Fig. 4

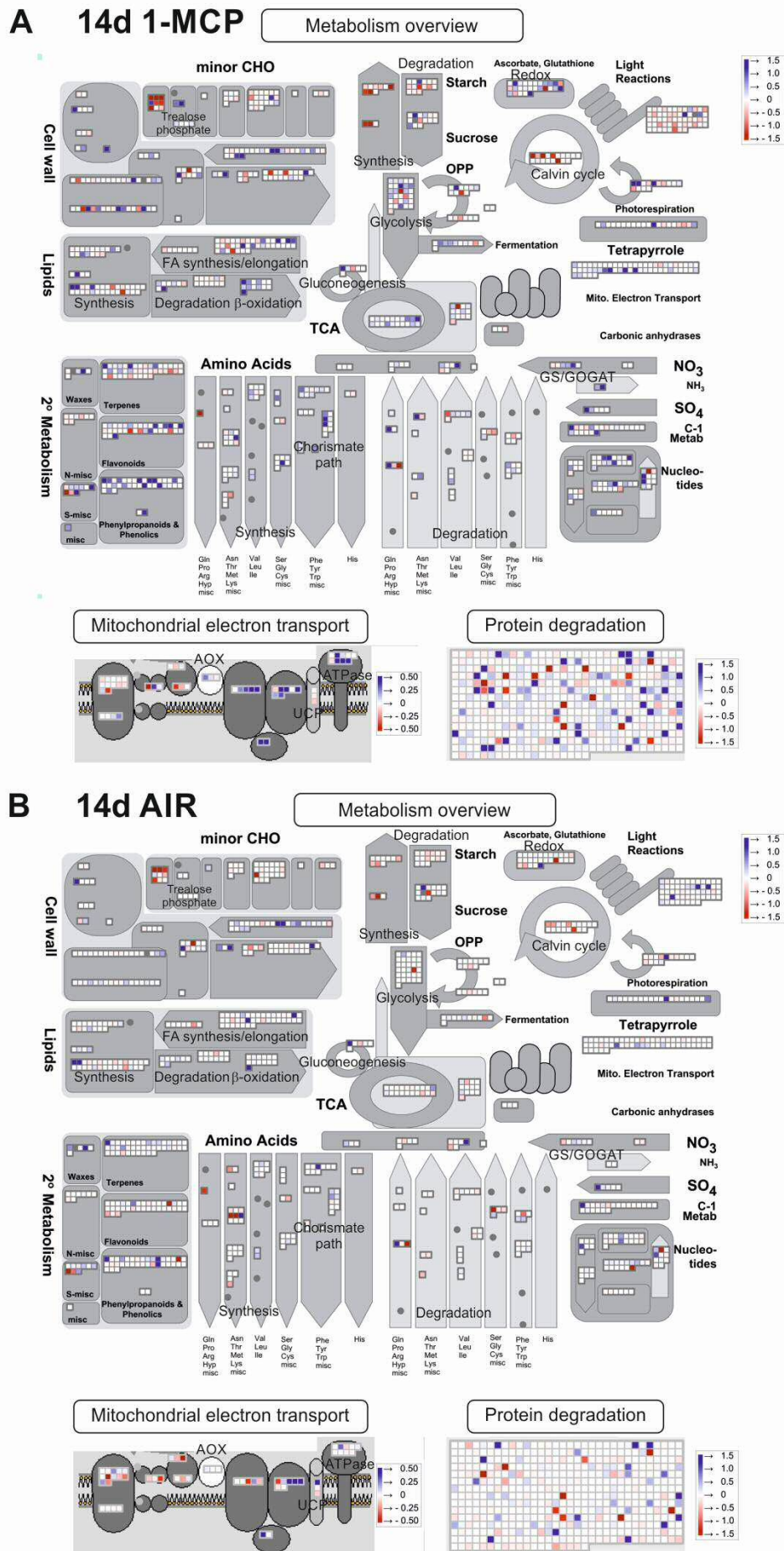


Figure 5

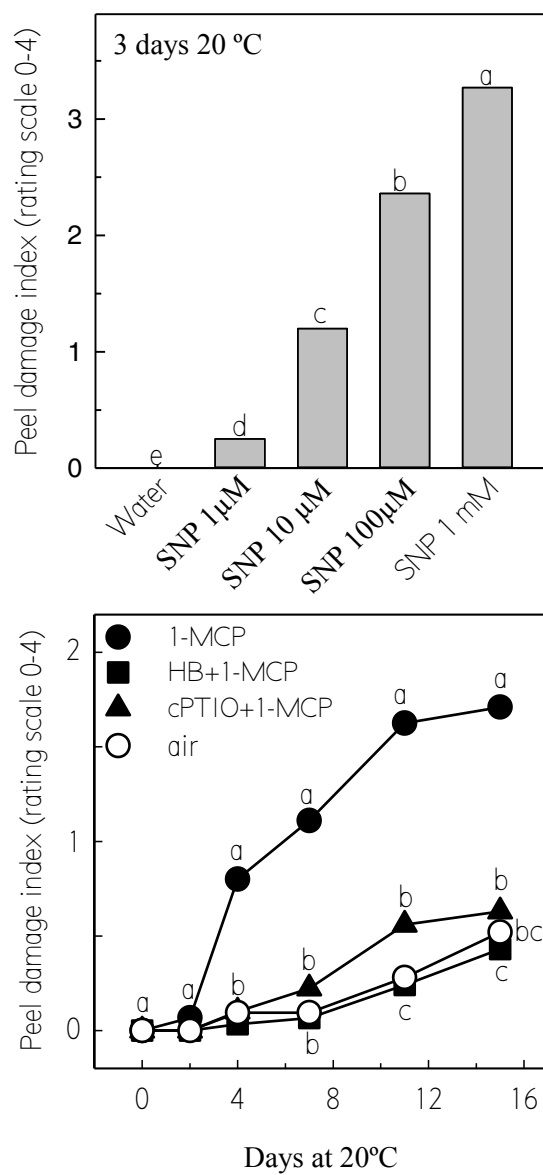
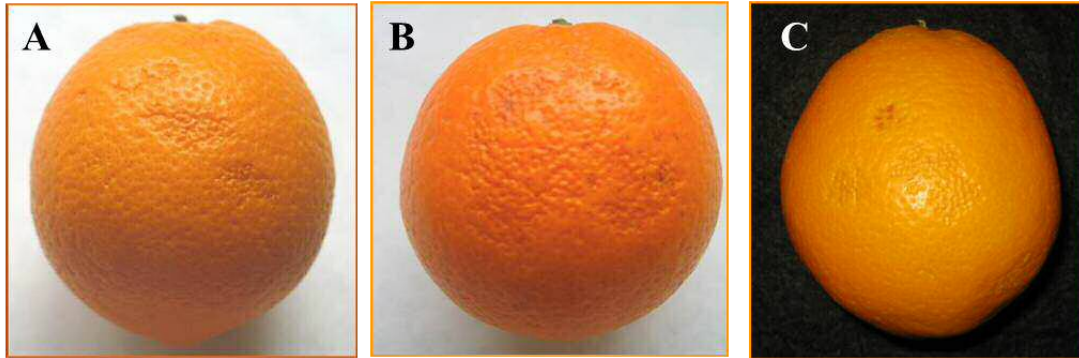


Figure 5.



Supplemental Fig. S1. Nonchilling peel pitting (NCP) syndrome in fruit held in air (A), and in fruits pretreated with 1-MCP (B) and SNP (C).

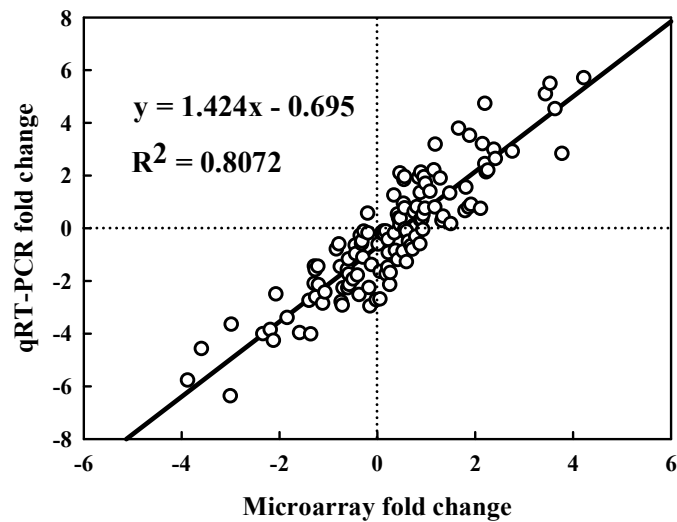


Fig. S2. Correlation in the expression of selected genes (Table S1) quantified using either the 12k citrus microarray or RT-qPCR. The expression of these genes was quantified in the flavedo and albedo of AC, EC and 1-MCP-treated fruits stored for 4 and 14 days at 20 °C ($r^2 = 0.807$, $p \leq 0.05$).

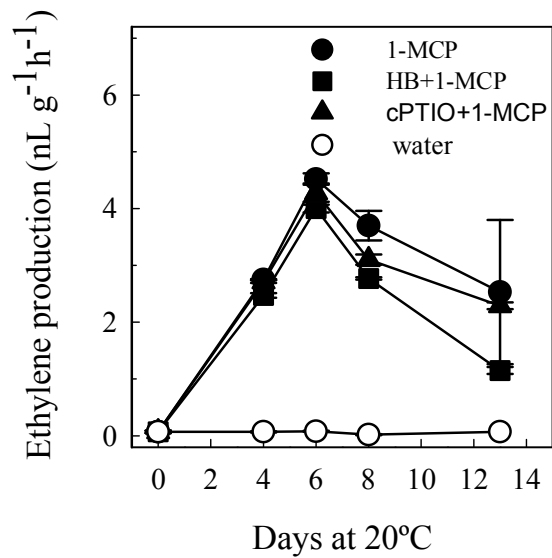


Fig. S3. Effect of HB (■) and cPTIO (▲) on the ethylene production of fruits treated with 1-MCP (●) and stored at 20 °C. No significant differences were found among mean values of these samples for the same storage period ($p \leq 0.05$) according to Tukey's test, and the values always differed significantly from the means of fruits treated only with water (○).

Table S1. Selected genes and primers used for comparison between the Citrus 12 k microarray and RT-qPCR gene expression data. Reference genes *CsACT*, *CsEF1 α* , and *CsTUB* were used for data normalization.

Gene	Citrus code	Most similar protein	Homolog in <i>A. thaliana</i>	Forward / Reverse	Sequence 5' → 3'	Amplicon size (pb)
<i>CsiACO1</i>	<i>orange1.lg020953m</i>	ACC oxidase 1	At1g05010	F	GCGGCTATCTTGGAGAAGATCAACGAGG	148
				R	GCCCTGCTTGAACAAGCTC	
<i>CsiCSC1</i>	<i>orange1.lg021775m</i>	Cysteine Synthase C1 (β -Cyanoalanine Synthase)	At3g61440	F	GCAGCGAACCCATGTTGATGAG	256
				R	GGCCACTGCTGGTCTGTCC	
<i>CsiERL1</i>	<i>orange1.lg004636m</i>	Ethylene Receptor-Like 1	At2g40940	F	CCGGAGCACTCAAATGATTC	141
				R	CCGTCATTACATCACATCCCAGG	
<i>CsiGDP</i>	<i>orange1.lg001531m</i>	Glycine Dehydrogenase Protein (Victorin Binding Protein)	At4g33010	F	GCCTGGTTAATGAGTCCAAGC	229
				R	GCCTCAACAGAAATGCCTCG	
<i>CsiGST1</i>	<i>orange1.lg027524m</i>	Glutathione S Transferase	At2g29420	F	GGGAGCTGCTGTTTGG	244
				R	CACGCGTGCAAGCCTGG	
<i>CsiSPS</i>	<i>orange1.lg001705m</i>	Sucrose-Phosphate Synthase	At4g10120	F	GCATGCATGGATTGGTGCGTGG	147
				R	GCTAGAATCTACTTCCGGTGAGGC	
<i>CsiACT</i>	<i>orange1.lg017088m</i>	Actin7. Structural constituent	AT5G09810	F	TTAACCCCAAGGCCAACAGA	176
				R	TCCCTCATAGATTGGTACAGTATGAGA	
<i>CsiEF1 α</i>	<i>orange1.lg010310m</i>	Translation elongation factor EF1A	AT1G18070	F	ATTGACAAGCGTGTGATTGAGC	171
				R	TCCACAAGGCAATATCAATGGTA	
<i>CsiTUB</i>	<i>orange1.lg013335m</i>	Tubulin1. Structural constituent	AT1G75780	F	GCATCTTGAACCCGGTAC	158
				R	ATCAATTCGGCGCCTTCAG	

Table S2. Expression levels of citrus genes in the flavedo (F) and albedo (A) tissues of AC, EC and 1-MCP-treated fruit stored for 4 and 14 days at 20 °C grouped according to the biological processes they belong to. Numbers in bold indicate statistically significant differences (SAM, FDR <0.05)

Biological Process		GO Level		Comparison vs Freshly Harvested (FH)									
RESPONSE TO HIPOXIA		5		4 days					14 days				
Gene Description	Homolog in <i>A. thaliana</i>	Log2 (AC/FH)		Log2 (EC/FH)		Log ₂ (MCP/FH)		Log2 (AC/FH)		Log2 (EC/FH)		Log ₂ (MCP/FH)	
		Flavedo	Albedo	Flavedo	Albedo	Flavedo	Albedo	Flavedo	Albedo	Flavedo	Albedo	Flavedo	Albedo
Non-symbiotic hemoglobin 1	AT2G16060	-0.387	+	1.076	+	0.116	+	-1.302	+	-	+	0.705	+
Hemoglobin II	AT2G16060	-0.096	0.874	1.262	1.800	0.735	1.407	-0.246	1.364	-0.288	1.380	0.818	2.818
Phytoalexin-deficient 4-2 protein	AT3G52430	0.606	0.640	0.940	0.833	-0.075	-0.125	-0.086	0.378	0.187	0.237	0.592	1.546
Pyruvate decarboxylase isozyme 1	AT5G54960	-0.119	0.081	0.279	0.523	0.445	0.332	0.208	0.249	0.272	0.273	0.490	0.702
2-on-2 hemoglobin	AT4G32690	0.458	0.314	0.777	0.654	0.508	0.435	0.451	0.453	0.509	0.363	0.665	0.683
F18C1.18 protein	AT3G05550	0.092	0.458	0.613	0.945	-0.015	-0.083	-0.138	0.293	-0.112	0.352	0.020	0.339

Biological Process		GO Level		Comparison vs FH									
Response to toxin		4		4 days					14 days				
Gene Description	Homolog in <i>A. thaliana</i>	Log2 (AC/FH)		Log2 (EC/FH)		Log ₂ (MCP/FH)		Log2 (AC/FH)		Log2 (EC/FH)		Log ₂ (MCP/FH)	
		Flavedo	Albedo	Flavedo	Albedo	Flavedo	Albedo	Flavedo	Albedo	Flavedo	Albedo	Flavedo	Albedo
Glutathione S-transferase	At1g10360		0.225	+	-		-		-		-	+	-
Glutathione S-transferase	At2g29420	0.859	-0.105	1.416	0.533	1.024	1.107	0.248	0.081	0.460	0.253	1.051	3.802
Glutathione S-transferase	At2g29420	0.767	0.185	1.664	0.697	1.317	1.508	0.342	0.484	0.584	0.236	1.178	3.667
Beta-cyanoalanine synthase	At3g61440	1.656	4.227	2.181	4.510	-1.911	-1.491	-0.952	0.890	-1.958	0.662	2.182	2.917
Putative glutathione S-transferase T3	At2g29420	0.252	0.173	0.552	0.540	1.068	1.158	0.111	0.381	0.202	0.654	1.383	2.896
Glutathione S-transferase GST 22	At2g30860	0.523	1.369	0.429	1.424	1.345	1.891	0.537	1.195	0.445	1.143	1.398	2.618
Glutathione S-transferase GST 22	At2g30860	0.532	1.036	0.288	1.063	1.166	1.423	0.549	0.768	0.467	0.920	1.274	2.270
Glutathione S-transferase GST 22	At2g30870	0.384	1.034	0.263	1.068	0.887	1.501	0.129	0.866	0.031	0.858	1.142	2.214
Hydroquinone glucosyltransferase	At4g01070	0.433	-0.476	1.064	0.125	0.325	0.217	1.030	0.549	1.193	0.628	1.033	1.764
Hydroquinone glucosyltransferase	At4g01070	0.285	-0.300	0.708	0.208	0.421	0.543	1.192	0.661	1.210	0.737	1.156	1.695
Glutathione S-transferase GST 14	At2g29420	0.709	0.608	0.560	0.619	0.955	0.905	0.529	0.355	0.459	0.326	0.913	1.429
Glutathione S-transferase	At2g29420	0.802	0.322	0.908	0.430	0.869	0.748	0.329	0.277	0.517	0.355	0.916	1.393
Nitrilase 4	At5g22300	0.677	1.124	0.454	1.166	0.289	0.378	0.416	0.729	0.377	0.790	1.166	1.207

Biological Process		GO Level		Comparison vs Fresly Harvested (FH)									
RESPONSE TO ETHYLELE STIMULUS		6		4 days					14 days				
Gene Description	Homolog in <i>A. thaliana</i>	Log2 (AC/FH)		Log2 (EC/FH)		Log ₂ (MCP/FH)		Log2 (AC/FH)		Log2 (EC/FH)		Log ₂ (MCP/FH)	
		Flavedo	Albedo	Flavedo	Albedo	Flavedo	Albedo	Flavedo	Albedo	Flavedo	Albedo	Flavedo	Albedo
WRKY transcription factor 6	At1g62300	0.596	1.199	1.230	1.832	-0.106	0.596	-0.555	1.085	-0.375	0.906	0.610	2.170
MYB6	At4g37260	1.312	0.795	1.279	1.433	1.384	0.934	0.746	0.709	0.938	0.982	1.677	1.767
Putative ethylene receptor expressed protein	At2g40940	0.734	1.620	0.399	0.991	0.852	0.450	0.547	0.312	0.509	0.585	1.488	1.719
	At2g26070	0.588	1.253	0.239	0.239	0.375	0.088	0.120	0.163	-0.082	0.114	0.994	1.256
Ethylene-responsive factor-like protein	At3g16770	0.305	0.180	0.853	0.860	0.573	0.300	0.567	1.063	0.798	1.282	1.041	1.206
G protein beta subunit	At4g34460	0.248	0.206	-0.184	0.216	0.299	-0.617	0.469	0.174	0.336	0.326	0.740	0.936
Transcription factor Myb1	At3g23250	0.551	0.300	0.529	0.339	0.539	0.201	0.700	0.367	0.423	0.263	1.195	0.626
Pathogenesis-related genes transcription factor	At4g11140	0.242	0.437	-0.035	-0.096	0.599	0.657	0.390	0.232	0.438	0.340	0.456	0.517
EIN3-like protein	At2g27050	0.321	0.670	-0.158	0.401	0.392	0.199	0.438	0.358	0.318	0.664	0.991	0.365
AP2/EREBP transcription factor ERF-2	At3g16770	0.227	0.598	0.037	-0.009	0.362	0.151	0.410	0.337	0.381	0.560	0.686	0.255
Anthranilate synthase beta subunit	At1g25220	0.647	0.529	1.147	0.883	-0.119	-0.232	0.152	0.146	0.112	-0.056	1.126	0.059

Biological Process		GO Level		Comparison vs Fresly Harvested (FH)									
OXYLIPIN METABOLIC PROCESS		9		4 days					14 days				
Gene Description	Homolog in <i>A. thaliana</i>	Log2 (AC/FH)		Log2 (EC/FH)		Log ₂ (MCP/FH)		Log2 (AC/FH)		Log2 (EC/FH)		Log ₂ (MCP/FH)	
		Flavedo	Albedo	Flavedo	Albedo	Flavedo	Albedo	Flavedo	Albedo	Flavedo	Albedo	Flavedo	Albedo
Lipoxygenase LOX1	AT3G45140	1.212	+	1.353	+	1.875	+	2.104	+	2.382	+	0.184	+
4-coumarate-CoA ligase-like protein	AT4G05160	0.011	-0.346	1.120	0.696	-0.403	-0.032	-0.713	-0.333	-0.516	-0.558	-0.146	1.444
12-oxophytodienoate reductase	AT2G06050	0.602	0.260	0.775	0.617	-0.189	-0.396	0.435	-0.049	0.171	0.151	0.468	0.907
Caffeine synthase	AT1G19640	0.240	0.111	1.120	0.403	1.295	0.863	-0.268	0.242	-0.386	0.217	0.011	0.772
Allene oxide synthase	AT5G42650	0.457	0.923	0.878	1.193	-0.134	0.191	0.416	0.473	0.427	0.965	0.739	0.729
SAMT	AT1G19640	0.163	-0.145	0.818	0.014	0.640	0.182	-0.247	-0.032	-0.269	0.150	-0.127	0.281
Mangrin	AT1G13280	0.451	0.496	0.762	0.356	0.084	-0.123	0.432	0.348	0.281	0.245	0.464	0.248
Lipoxygenase LOX1	AT1G72520	1.427	-0.247	1.228	-0.216	1.434	1.308	2.520	0.410	2.411	1.682	-0.014	0.190
Lipoxygenase	AT1G17420	0.097	0.096	0.530	0.392	0.023	-0.090	0.018	0.072	0.022	0.181	0.311	0.176
Lipoxygenase	AT1G72520	0.094	0.055	0.354	0.108	0.105	0.039	0.366	0.242	0.343	0.256	0.269	0.170
Lipoxygenase	AT3G45140	1.564	-0.105	1.300	0.080	1.653	1.595	2.248	0.606	2.503	1.728	0.019	0.135
Lipoxygenase	AT1G72520	1.361	-0.546	1.077	-0.228	1.353	0.574	2.253	0.147	2.373	1.016	0.231	0.128
Lipoxygenase LOX1	AT1G17420	1.607	-0.202	1.434	0.021	1.608	-0.743	2.606	0.638	2.665	1.395	0.053	0.117
Lipoxygenase	AT3G45140	1.442	-0.170	1.393	0.270	1.621	1.729	2.022	0.743	2.397	1.836	-0.233	0.070
Allene oxide cyclase precursor	AT3G25780	0.635	-0.042	0.799	0.179	0.357	-0.113	1.380	0.377	1.059	0.440	0.046	-0.168
Mangrin	AT1G13280	0.224	0.257	0.596	0.225	-0.147	-0.342	0.217	-0.157	0.131	-0.273	0.150	-0.295

Biological Process		Comparison vs Freshly Harvested (FH)											
FATTY ACID BIOSYNTHETIC PROCESS		4 days						14 days					
Gene Description	Homolog in <i>A. thaliana</i>	Log2 (AC/FH)		Log2 (EC/FH)		Log ₂ (MCP/FH)		Log2 (AC/FH)		Log2 (EC/FH)		Log ₂ (MCP/FH)	
		Flavado	Albedo	Flavado	Albedo	Flavado	Albedo	Flavado	Albedo	Flavado	Albedo	Flavado	Albedo
Lipoxygenase LOX1	AT3G45140	1.212	+	1.353	+	1.875	+	2.104	+	2.382	+	0.184	+
Fiddlehead-like protein	AT2G26250	0.580	2.181	-0.439	0.465	0.928	1.076	1.692	2.392	0.641	2.036	0.999	1.639
4-coumarate-CoA ligase-like protein	AT4G05160	0.011	-0.346	1.120	0.696	-0.403	-0.032	-0.713	-0.333	-0.516	-0.558	-0.146	1.444
Homogentisate geranylgeranyl transfera	AT2G18950	0.638	-0.152	0.821	0.066	0.410	0.409	-0.093	-0.056	0.197	-0.108	0.728	0.940
12-oxophytodienoate reductase	AT2G06050	0.602	0.260	0.775	0.617	-0.189	-0.396	0.435	-0.049	0.171	0.151	0.468	0.907
no_annotation_available	AT2G18950	0.824	-0.465	1.353	-0.132	0.504	0.109	-0.878	-0.232	0.110	-0.234	1.240	0.780
Caffeine synthase	AT1G19640	0.240	0.111	1.120	0.403	1.295	0.863	-0.268	0.242	-0.386	0.217	0.011	0.772
Homogentisate geranylgeranyl transfera	AT2G18950	0.949	-0.365	0.927	-0.466	0.618	0.459	0.016	-0.045	0.546	0.425	1.055	0.758
Allene oxide synthase	AT5G42650	0.457	0.923	0.878	1.193	-0.134	0.191	0.416	0.473	0.427	0.965	0.739	0.729
Homogentisate geranylgeranyl transfera	AT2G18950	0.861	-0.357	1.152	0.140	0.451	0.377	-0.716	-0.179	0.243	-0.071	1.109	0.596
F18O14.21	AT1G19440	0.240	0.094	0.442	0.343	0.229	0.426	0.297	0.305	0.397	0.321	0.424	0.553
SAMT	AT1G19640	0.163	-0.145	0.818	0.014	0.640	0.182	-0.247	-0.032	-0.269	0.150	-0.127	0.281
Mangrin	AT1G13280	0.451	0.496	0.762	0.356	0.084	-0.123	0.432	0.348	0.281	0.245	0.464	0.248
Putative fatty acid elongase	AT2G28630	1.404	-0.481	-0.148	-0.609	0.736	0.420	2.092	0.030	0.639	0.167	1.834	0.209
Lipoxygenase LOX1	AT1G72520	1.427	-0.247	1.228	-0.216	1.434	1.308	2.520	0.410	2.411	1.682	-0.014	0.190
Chloroplast fatty acid desaturase 6	AT4G30950	0.335	-0.281	0.631	-0.197	0.202	-0.501	0.496	-0.095	0.349	0.168	-0.078	0.189
Putative fatty acid elongase	AT5G04530	0.836	-0.128	-0.365	-0.259	1.068	0.297	1.828	0.253	0.920	0.477	0.598	0.176
Lipoxygenase	AT1G17420	0.097	0.096	0.530	0.392	0.023	-0.090	0.018	0.072	0.022	0.181	0.311	0.176
Lipoxygenase	AT1G72520	0.094	0.055	0.354	0.108	0.105	0.039	0.366	0.242	0.343	0.256	0.269	0.170
Lipoxygenase	AT3G45140	1.564	-0.105	1.300	0.080	1.653	1.595	2.248	0.606	2.503	1.728	0.019	0.135
Lipoxygenase	AT1G72520	1.361	-0.546	1.077	-0.228	1.353	0.574	2.253	0.147	2.373	1.016	0.231	0.128
Lipoxygenase LOX1	AT1G17420	1.607	-0.202	1.434	0.021	1.608	-0.743	2.606	0.638	2.665	1.395	0.053	0.117
Lipoxygenase	AT3G45140	1.442	-0.170	1.393	0.270	1.621	1.729	2.022	0.743	2.397	1.836	-0.233	0.070
Omega-3 fatty acid desaturase	AT5G05580	0.564	0.177	0.814	0.564	-0.181	-0.627	0.655	0.023	0.354	-0.463	-0.098	-0.028
Allene oxide cyclase precursor	AT3G25780	0.635	-0.042	0.799	0.179	0.357	-0.113	1.380	0.377	1.059	0.440	0.046	-0.168
Protein At1g02190	AT1G02190	0.463	0.420	1.001	-0.486	-0.483	-0.184	0.153	0.773	0.082	0.682	-0.170	-0.212
Acyl carrier protein 1, chloroplast precu	AT4G25050	0.371	0.135	0.730	-0.044	-0.404	-0.281	0.547	-0.054	0.152	0.037	0.216	-0.238
T25K16.11	AT1G01120	1.266	-0.531	1.189	-0.412	0.445	-0.142	1.075	-0.517	0.506	0.173	1.117	-0.291
Mangrin	AT1G13280	0.224	0.257	0.596	0.225	-0.147	-0.342	0.217	-0.157	0.131	-0.273	0.150	-0.295
Enoyl-ACP reductase precursor	AT2G05990	0.173	0.226	0.652	0.189	-0.427	-0.175	0.260	-0.094	-0.079	-0.228	0.081	-0.510
Cuticle protein	AT5G57800	0.674	0.060	0.276	-0.777	-0.147	-0.192	0.959	0.680	0.920	0.723	0.536	-0.586

Biological Process		GO Level		Comparison vs Freshly Harvested (FH)									
PHOTOSYNTHESIS		4		4 days					14 days				
Gene Description	Homolog in <i>A. thaliana</i>	Log2 (AC/FH)		Log2 (EC/FH)		Log ₂ (MCP/FH)		Log2 (AC/FH)		Log2 (EC/FH)		Log ₂ (MCP/FH)	
		Flavado	Albedo	Flavado	Albedo	Flavado	Albedo	Flavado	Albedo	Flavado	Albedo	Flavado	Albedo
Chlorophyll a-b binding protein 8, chloro	AT1G61520	-	-0.117	0.084	-	-	-0.036	0.059	0.048	0.362	0.005	-0.164	-0.255
Photosystem I reaction center subunit V	AT1G52230	-0.388	-0.047	-0.693	-0.393	-0.036	0.160	0.137	0.223	-0.017	0.321	-0.422	-0.271
Ultraviolet-B-repressible protein	AT2G06520	-0.357	-0.361	-0.381	-0.490	-0.075	-0.095	-0.157	-0.224	0.188	-0.123	-0.758	-0.271
expressed protein	AT4G11960	-0.525	-0.432	-0.419	-0.681	-0.203	-0.720	0.306	-0.069	0.737	0.354	-0.371	-0.360
no_annotation_available	ATCG00510	0.033	-0.282	-0.296	-0.626	0.626	0.146	0.660	0.308	0.363	0.103	-0.012	-0.408
Serine/threonine-protein kinase SNT7, c	AT1G68830	-0.113	-0.173	-0.198	-0.597	0.045	-0.116	0.707	0.288	0.702	0.517	-0.061	-0.465
Chlorophyll a-b binding protein CP29.3, i	AT2G40100	-0.425	-0.126	-0.647	-0.820	0.442	-0.029	0.428	0.181	0.346	0.085	-0.286	-0.466
Photosystem II 5 kDa protein, chloroplas	AT3G21055	-1.324	-0.778	-0.976	-	-0.090	-1.403	-0.200	-0.203	-0.222	-0.125	-0.870	-0.494
Oxygen evolving enhancer protein 1 pre	AT3G50820	-0.858	-0.459	-1.622	-1.348	0.095	0.526	0.143	0.434	0.076	0.788	-1.479	-0.509
Photosystem I reaction center subunit V	AT1G55670	-0.285	-0.749	-0.571	-0.630	-0.143	-0.123	-0.130	-0.430	0.293	0.197	-0.805	-0.529
Ribulose biphosphate carboxylase smal	AT5G38410	-1.475	-0.936	-1.262	-0.763	-0.885	-0.556	-1.350	-0.773	-1.319	-0.665	-1.685	-0.719
Chloroplast photosystem II 10 kDa prote	AT1G79040	0.013	-0.318	-0.523	-0.645	0.207	-0.104	0.510	0.117	0.427	0.264	-0.523	-0.761
Photosystem I subunit XI	AT4G12800	0.202	0.706	-0.684	-0.260	0.160	0.431	0.949	1.188	0.495	1.283	-1.096	-0.797
ATP synthase delta chain, chloroplast pr	AT4G09650	-0.412	-0.389	-0.188	-0.480	-0.506	-0.413	0.025	0.079	0.307	-0.137	-0.375	-0.801
Cytochrome b6-f complex iron-sulfur sul	AT4G03280	-0.906	-0.479	-1.190	-0.943	-0.763	-0.489	0.028	-0.269	-0.048	0.089	-1.166	-0.829
Phosphoenolpyruvate carboxylase 2	AT1G53310	-1.383	-0.864	-0.860	-0.260	-1.360	-0.825	-1.892	-1.424	-2.035	-1.359	-1.312	-0.890
Chlorophyll a/b-binding protein	AT1G29910	-1.425	-1.093	-1.225	-1.073	-1.130	-0.877	-0.950	-0.828	-0.218	-0.186	-1.970	-0.902
Cell division protein ftsH homolog 1, chl	AT1G50250	-0.463	-0.308	-0.432	-0.455	-0.544	-0.430	-0.273	-0.389	-0.370	-0.426	-0.866	-0.976
NADH-plastoquinone oxidoreductase su	ATCG00440	-0.598	-0.462	-1.023	-0.613	-0.167	-0.146	0.076	-0.217	-0.393	-0.230	-0.939	-1.041
Photosystem II reaction center W protei	AT2G30570	-0.847	-1.023	-0.902	-1.345	-0.290	-0.218	0.343	0.077	0.290	0.313	-1.122	-1.093
Glyceraldehyde-3-phosphate dehydroge	AT1G42970	-0.994	-1.223	-0.756	-1.115	-0.251	-0.443	-0.108	-0.802	-0.085	-0.338	-1.327	-1.228
Chloroplast protease precursor	AT2G30950	-0.797	-0.294	-0.976	-0.751	-1.036	-1.047	-0.750	-0.818	-0.922	-0.499	-1.163	-1.627
CP12 precursor	AT3G62410	-1.455	-1.937	-1.530	-2.167	-0.958	-1.089	-0.860	-0.799	-0.710	-0.379	-2.686	-2.334
Phosphoribulokinase, chloroplast precu	AT1G32060	-1.133	-1.173	-1.389	-1.882	-1.057	-1.403	-0.239	-1.202	-0.034	-1.275	-1.652	-2.636

Cellular component		GO Level		Comparison vs Fresly Harvested									
PLASMA MEMBRANE		5		4 days					14 days				
Gene Description	Homolog in <i>A. thaliana</i>	Log2 (AC/FH)		Log2 (EC/FH)		Log ₂ (MCP/FH)		Log2 (AC/FH)		Log2 (EC/FH)		Log ₂ (MCP/FH)	
		Flavado	Albedo	Flavado	Albedo	Flavado	Albedo	Flavado	Albedo	Flavado	Albedo	Flavado	Albedo
LRR receptor-like protein kinase	AT1G66150	-0.158	+	-0.035	+	-0.469	+	0.007	+	-0.230	+	-0.222	+
Seven transmembrane protein Mlo4	AT1G11000	-0.333	+	0.138		-	+	1.035	+	1.865	+	-	+
Non-symbiotic hemoglobin 1	AT2G16060	-0.387	+	1.076	+	0.116	+	-1.302	+	-	+	0.705	+
no_annotation_available	AT2G26570	-0.229	+	-0.394	+	-0.398	+	-	+	-	+	-0.363	+
UPI00004DA1E9; LOC395048 protein	AT3G54960	0.122	+	0.280	+	0.324	+	0.320	+	0.257	+	0.721	+
Putative mitochondrial processing pepti	AT3G16480	-0.169	+	-0.261	+	-0.102	+	0.118	+	-0.168	+	-0.207	+
no_annotation_available	AT4G21380	0.538	+	0.236	+	0.327	+	1.058	+	1.165	+	0.480	+
Cellulose synthase	AT4G32410	0.169	+	-0.034	+	0.271	+	0.243	+	0.496	+	0.033	+
Phosphatidylinositol transfer-like protei	AT4G39170	-0.069	+	-0.056	+	0.032	+	0.088	+	0.154	+	0.215	+
RIB40 genomic DNA, SC003	AT4G31700	-0.029	+	-0.244	+	-	+	-	+	-1.348	+	0.020	+
Secreted glycoprotein 3	AT4G21380	0.082	+	-0.288	+	-0.281	+	-0.123	+	-0.136	+	0.663	+
ENSANGP0000000953	AT5G10940	0.497	+	0.215	+	0.326	+	0.643	+	0.346	+	0.746	+
Elongation factor 1-alpha	AT5G60390	+					+						+
40S ribosome protein S5	AT2G37270	0.334	2.254	1.459	3.860	-0.514	2.054	0.072	2.577	0.663	2.530	1.775	4.196
Receptor-like protein kinase	AT2G31880	-0.324	1.617	-0.091	2.653	0.120	2.692	-2.775	2.564	0.093	2.501	0.578	3.845
Eugenol O-methyltransferase	AT5G54160	0.036	-0.256	1.532	1.282	0.095	0.488	-0.773	-0.281	-0.199	-0.019	3.692	3.837
Multidrug resistance-associated protein	AT3G13080	0.300	-0.113	0.726	0.836	0.843	1.689	-0.464	-0.062	0.160	0.166	1.083	3.227
Dicyanin	AT5G20230	0.480	0.023	2.493	1.564	-0.098	1.176	-0.353	0.199	0.671	0.432	2.052	2.960
Catechol O-methyltransferase	AT5G54160	0.929	0.345	1.735	1.542	0.635	0.886	0.378	-0.060	0.560	-0.025	3.019	2.932
Caffeic acid 3-O-methyltransferase	AT5G54160	0.541	1.076	1.153	0.978	0.698	1.448	-0.797	0.116	-0.306	-0.205	1.882	2.880
Hemoglobin II	AT2G16060	-0.096	0.874	1.262	1.800	0.735	1.407	-0.246	1.364	-0.288	1.380	0.818	2.818
no_annotation_available	AT3G02600	-0.402	-0.057	0.429	0.943	0.234	1.135	-0.563	0.669	-0.409	0.621	0.431	2.684
CYP81E8	AT4G37370	0.927	1.973	0.624	1.670	1.925	2.001	1.007	0.866	0.906	1.031	2.236	2.638
Glutathione S-transferase GST 22	AT2G30860	0.523	1.369	0.429	1.424	1.345	1.891	0.537	1.195	0.445	1.143	1.398	2.618
AT4g08850/T32A17_160	AT4G08850	0.191	0.072	0.665	0.679	0.358	0.566	0.023	0.438	0.398	0.573	1.073	2.538
Receptor-like protein kinase	AT2G31880	0.278	0.134	0.349	1.018	0.616	1.078	0.466	1.194	0.207	1.261	1.214	2.475
Receptor-like protein kinase	AT2G31880	-0.074	-0.289	0.007	0.251	0.347	1.051	-0.361	0.705	-0.105	0.891	0.854	2.471
Serine/threonine-protein phosphatase E	AT2G27210	1.986	0.672	2.854	2.064	0.654	0.236	1.728	0.555	2.049	0.626	2.919	2.433
Sulfate adenyltransferase	AT3G22890	1.118	1.253	1.445	1.828	1.106	0.948	1.552	1.338	1.045	1.577	2.433	2.421
Ascorbate peroxidase	AT1G07890	0.521	0.000	0.597	0.056	0.610	0.738	0.670	0.325	0.802	0.890	1.500	2.382
Genomic DNA, chromosome 5, TAC clon	AT5G52450	0.426	0.271	0.733	0.884	0.736	0.760	0.522	-0.034	-0.101	-0.052	1.850	2.362
OSJNBa0010D21.1 protein	AT3G24240	-0.315	-0.439	0.111	-0.208	0.429	0.310	-0.155	-0.204	0.292	-0.043	1.179	2.308
Glutathione S-transferase GST 22	AT2G30860	0.532	1.036	0.288	1.063	1.166	1.423	0.549	0.768	0.467	0.920	1.274	2.270
Glutathione S-transferase GST 22	AT2G30860	0.384	1.034	0.263	1.068	0.887	1.501	0.129	0.866	0.031	0.858	1.142	2.214
Putative quinone oxidoreductase	AT4G27270	-0.245	0.103	0.252	0.319	-0.291	0.084	-0.628	-0.163	-0.548	-0.363	1.054	2.188

P-glycoprotein-like proetin	AT3G62150	0.091	0.987	0.631	1.542	0.195	1.596	0.278	1.570	0.313	1.275	0.731	2.165
Cinnamyl alcohol dehydrogenase	AT5G19440	1.029	1.296	1.599	1.946	0.527	0.403	0.895	0.564	0.819	0.970	1.934	2.102
Putative exostoses	AT5G04500	0.210	1.046	0.403	1.390	0.782	1.185	0.457	1.655	0.173	1.305	1.388	2.040
Chitinase precursor	AT3G12500	-0.085	0.101	0.381	0.375	0.063	0.327	-0.192	0.405	-0.236	0.191	0.058	2.033
F10B6.27	AT1G14870	-0.111	0.319	0.428	0.342	0.252	0.547	-0.367	0.580	-0.539	0.436	0.963	1.960
40S ribosomal protein S18	AT4G09800	0.342	0.189	1.012	1.415	-0.426	0.165	-0.216	0.427	0.345	0.507	0.974	1.924
Putative exostoses	AT5G04500	0.265	0.836	0.341	1.167	0.625	0.990	0.573	1.225	0.459	1.271	1.370	1.923
Adenine phosphoribosyltransferase-like	AT1G27450	1.007	1.335	1.174	1.796	0.134	0.598	0.621	0.917	0.198	0.729	1.595	1.882
Sugar transport protein 14	AT1G77210	0.046	-0.675	0.203	-0.527	0.188	-0.048	-0.132	-0.487	0.095	-0.558	1.127	1.842
Putative xyloglucan endotransglycosylas	AT4G30270	-0.042	-0.769	0.506	0.763	-0.079	0.224	-1.988	0.335	-1.389	0.139	1.155	1.828
Pyridoxine biosynthesis protein	AT5G01410	0.262	0.966	0.147	1.035	0.277	0.797	0.215	0.735	-0.040	1.089	0.984	1.824
T1N24.22 protein	AT5G25930	0.291	0.911	0.824	1.233	0.228	1.306	0.309	1.075	0.209	0.982	0.876	1.789
Receptor-like protein kinase	AT2G31880	0.103	-0.196	0.187	0.619	0.509	0.805	-0.040	0.624	0.254	0.698	0.812	1.766
OSJNBa0021F22.13 protein	AT3G47570	-0.017	-0.269	-0.094	-0.270	1.005	0.638	0.390	0.420	0.501	0.487	1.198	1.701
Inorganic phosphate transporter 1-4 (At no_annotation_available	AT2G38940	0.498	0.175	0.575	0.834	0.389	1.139	0.482	0.173	0.272	0.340	0.028	1.635
	AT1G34320	0.826	0.289	1.493	1.607	0.074	0.057	0.710	0.388	1.242	0.438	1.211	1.622
Receptor kinase Lecrk	AT2G37710	0.245	0.699	0.209	0.817	0.617	0.912	0.386	0.711	0.341	0.737	1.100	1.573
Adenosine kinase 2	AT5G03300	0.313	0.318	1.081	1.279	-0.414	-0.031	-0.399	-0.391	-0.425	-0.377	1.252	1.559
Caffeic acid 3-O-methyltransferase 1	AT5G54160	0.149	0.536	0.403	0.567	0.320	0.750	-0.473	0.084	-0.535	-0.033	0.539	1.539
Glutamine synthetase	AT5G37600	0.638	1.033	0.941	1.279	0.226	0.586	0.395	0.518	0.209	0.501	1.026	1.509
no_annotation_available	AT2G46330	-0.107	0.437	0.574	1.525	0.245	1.097	-1.438	1.301	-1.189	1.055	0.188	1.470
NADP-dependent isocitrate dehydrogen	AT1G65930	0.474	0.646	0.532	0.402	0.632	0.663	1.191	0.749	1.288	1.581	0.980	1.413
Putative bacterial blight resistance prote	AT3G49670	0.145	-0.483	-0.065	-0.122	0.972	1.164	0.544	0.132	0.096	0.244	0.758	1.398
Putative ABC transporter; 66585-65723 no_annotation_available	AT1G67940	-0.093	1.070	-0.372	1.267	0.314	0.307	0.124	0.996	0.083	0.827	1.540	1.393
	AT4G35470	0.225	0.141	-0.063	0.536	0.730	1.215	0.822	0.632	0.489	0.596	0.847	1.372
Multidrug resistance-associated protein	AT3G21250	-0.057	-0.057	0.438	0.409	-0.218	0.190	-0.348	-0.152	-0.074	-0.016	0.976	1.350
Putative serine/threonine-specific prote	AT2G33580	0.267	0.231	0.393	0.505	0.595	0.631	0.164	0.474	0.283	0.431	0.908	1.305
Integral membrane protein, putative	AT3G21690	0.202	0.705	0.708	1.359	0.286	0.602	-0.515	0.212	-0.327	0.366	1.132	1.298
Receptor-like protein kinase	AT5G48380	0.182	0.105	0.038	0.339	0.509	1.010	0.031	0.285	-0.011	0.615	0.505	1.294
VDAC2.1	AT5G67500	0.231	0.494	0.340	0.565	0.322	0.653	0.197	0.260	0.129	0.177	0.643	1.254
Adenine phosphoribosyltransferase-like	AT1G27450	0.804	0.828	0.797	1.094	0.237	0.231	0.637	0.511	0.354	0.561	1.423	1.221
SNAP25 homologous protein SNAP33	AT5G61210	0.013	0.209	0.215	0.605	0.109	0.545	-0.094	0.355	-0.307	0.260	0.169	1.216
Putative peptide transport protein	AT3G54140	0.077	0.239	0.178	0.350	0.142	0.385	0.345	-0.006	0.433	0.432	0.736	1.214
5-methyltetrahydropteroyltriglutamate- Nitrilase 4	AT5G17920	0.335	0.514	0.295	0.554	0.172	0.380	-0.068	-0.592	-0.366	-0.291	0.815	1.209
	AT5G22300	0.677	1.124	0.454	1.166	0.289	0.378	0.416	0.729	0.377	0.790	1.166	1.207
Protein kinase domain, putative	AT4G21380	0.184	0.129	0.242	0.338	0.318	0.328	0.398	0.127	0.547	0.332	0.799	1.205
Allyl alcohol dehydrogenase	AT5G16990	-0.010	-0.232	0.210	0.101	0.331	0.495	0.502	0.147	0.459	0.256	0.084	1.204
Adenylate kinase, putative	AT5G50370	0.605	0.876	0.667	1.628	0.248	0.716	0.056	0.563	-0.192	0.631	0.521	1.202
F9L1.11 protein	AT1G71140	-0.046	0.106	-0.035	0.240	0.095	0.583	-0.299	-0.120	-0.272	-0.044	0.091	1.200
RING/C3HC4/PHD zinc finger-like protei	AT3G05200	0.188	0.183	0.404	0.804	0.253	0.476	-0.516	0.797	-0.490	0.933	0.364	1.199
40S ribosomal protein S5	AT3G11940	0.300	0.124	0.747	1.221	-0.325	-0.849	0.394	0.338	0.317	0.254	0.498	1.198
Glutamate dehydrogenase 2	AT5G07440	-0.293	0.012	-0.009	0.216	0.146	0.183	-0.156	-0.212	-0.208	-0.311	0.514	1.187

Cysteine protease	AT4G35350	-0.106	-0.271	-0.051	0.082	-0.082	-0.214	-0.223	-0.071	0.050	-0.162	0.503	1.186
ADP,ATP carrier protein 1, mitochondria	AT3G08580	0.303	0.440	0.152	0.602	0.381	0.603	0.720	0.182	0.124	0.462	0.453	1.164
Secreted glycoprotein 3	AT4G21380	-0.094	-0.100	0.190	0.497	0.026	0.309	-0.045	0.341	0.097	0.293	0.313	1.146
Sucrose synthase	AT3G43190	0.312	0.291	0.232	0.364	0.349	0.226	0.636	0.265	0.288	0.331	0.660	1.104
5-methyltetrahydropteroyltriglutamate-	AT5G17920	0.169	0.443	0.218	0.337	0.436	0.511	-0.105	-0.052	0.107	-0.046	0.631	1.097
Hexose transporter	AT1G11260	0.184	-0.065	0.230	0.109	0.353	0.693	0.241	0.036	0.182	0.040	0.305	1.091
Putative receptor protein kinase PERK1	AT2G33580	0.222	0.434	0.366	0.311	0.433	0.452	0.360	0.660	0.476	0.848	0.907	1.082
Receptor-protein kinase-like protein	AT3G51550	0.264	0.498	0.327	0.469	0.450	0.380	0.576	0.646	0.631	0.790	0.915	1.066
Nodulin26-like major intrinsic protein	AT4G18910	1.676	0.338	1.381	0.188	2.238	0.581	1.097	0.177	1.671	0.255	1.247	1.054
Receptor-like protein kinase	AT5G48380	0.217	0.023	0.072	0.235	0.571	0.693	-0.052	0.080	-0.057	0.192	0.583	1.052
S glycoprotein	AT4G21380	0.132	-0.112	0.170	0.275	0.281	0.143	0.403	0.395	0.306	0.313	0.664	1.044
Receptor-protein kinase-like protein	AT3G51550	-0.082	-0.344	0.155	-0.014	0.439	0.776	-0.184	-0.005	-0.272	-0.049	0.187	1.042
PDR6 ABC transporter	AT2G36380	0.394	0.271	0.252	0.383	0.761	1.140	0.472	1.008	0.160	0.689	0.345	1.034
Wall-associated kinase, putative	AT1G25390	0.194	-0.328	0.019	0.205	0.255	-0.120	0.020	-0.089	0.068	0.191	0.461	1.030
T17B22.4 protein	AT3G03270	-0.391	-0.198	-0.020	0.024	-1.100	-0.377	-1.341	-0.556	-1.081	-0.630	-0.417	1.029
expressed protein	AT5G12010	-0.360	-0.513	0.373	0.274	0.025	0.270	0.154	0.388	0.124	0.198	0.172	1.018
LEM3-like	AT1G79450	0.284	0.369	0.168	0.548	0.356	0.539	0.130	0.443	-0.017	0.422	0.480	1.011
Putative wall-associated kinase 2	AT1G21240	0.003	-0.089	0.126	0.173	0.264	0.428	0.311	0.386	0.297	0.289	0.385	0.989
Gb AAD56319.1	AT5G41330	0.004	0.091	0.532	0.998	0.518	0.816	-0.285	1.001	0.111	0.634	0.221	0.985
F15H18.11	AT1G18390	0.105	-0.033	0.150	0.353	0.133	0.107	0.179	0.290	0.282	0.263	0.306	0.970
Armadillo repeat-containing protein	AT1G76390	0.380	0.556	0.368	0.559	0.322	0.387	0.093	0.447	0.200	0.539	0.740	0.969
Glucose-6-phosphate/phosphate-translc	AT1G61800	0.464	0.248	0.575	0.776	0.110	0.109	0.313	-0.010	0.190	-0.012	0.757	0.962
Glyceraldehyde-3-phosphate dehydroge	AT3G04120	-0.153	0.117	-0.080	0.174	0.010	0.401	0.027	0.292	0.068	0.326	0.248	0.960
Putative ABC transporter	AT1G17840	0.858	-0.153	1.090	0.417	0.196	-0.567	1.475	-0.882	1.629	-0.230	0.789	0.958
Pto kinase interactor 1	AT1G48210	-0.355	-0.207	0.182	0.043	0.196	0.611	-0.177	-0.070	-0.190	-0.044	0.282	0.945
AT4g26970/F10M23_310	AT2G05710	0.268	0.186	0.193	0.508	0.298	0.537	0.607	0.205	0.161	0.560	0.773	0.936
G protein beta subunit	AT4G34460	0.248	0.206	-0.184	0.216	0.299	-0.617	0.469	0.174	0.336	0.326	0.740	0.936
Cytochrome b5 isoform Cb5-A	AT5G53560	0.365	0.045	0.151	0.160	0.162	0.109	0.044	-0.200	0.116	-0.149	0.373	0.936
MAP kinase phosphatase 1	AT3G06110	0.115	0.007	0.022	0.051	0.545	0.738	0.256	0.375	0.120	0.409	0.251	0.935
At2g25260	AT5G25265	0.257	0.437	0.339	0.598	-0.013	-0.062	-0.198	-0.031	-0.073	-0.091	0.479	0.929
Synaptobrevin-like protein	AT2G33120	-0.033	0.274	-0.063	0.274	0.427	0.636	0.177	0.679	0.088	0.712	0.353	0.927
Putative leucine-rich repeat receptor kir	AT2G16250	-0.414	-0.224	-0.127	-0.076	0.034	0.126	-0.498	-0.240	-0.689	-0.137	-0.306	0.919
Thiolase, putative	AT2G33150	0.159	0.050	0.268	0.352	0.249	0.213	0.258	0.003	0.055	0.094	0.496	0.915
Ammonium transporter	AT4G13510	0.152	0.351	0.740	0.348	0.135	0.414	0.451	0.123	0.040	0.187	0.588	0.912
At2g31880/F20M17.8	AT2G31880	0.099	0.251	-0.086	0.101	0.056	0.036	-0.267	0.156	-0.152	0.576	0.365	0.907
Putative acyl-CoA synthetase	AT4G23850	-0.148	0.084	0.090	0.169	0.020	0.065	-0.005	-0.095	-0.057	0.078	0.476	0.905
Adenylate kinase B	AT5G50370	0.155	0.140	0.068	0.065	0.103	0.145	0.209	0.134	0.096	0.394	0.299	0.905
Seed maturation protein PM37	AT3G44110	0.379	0.743	-0.023	0.188	0.626	0.723	1.150	1.094	1.166	1.738	0.896	0.898
no_annotation_available	AT4G35310	0.128	0.039	0.237	0.726	0.690	0.809	-0.078	0.113	-0.365	-0.149	0.634	0.885
Cytochrome P450 monooxygenase CYP8	AT4G31500	-0.001	-0.391	0.034	0.092	0.167	0.499	1.782	1.969	1.647	1.501	0.183	0.882
NOI protein, nitrate-induced	AT5G55850	-0.249	0.265	-0.045	0.355	-0.185	0.116	-0.492	0.015	-0.560	0.230	0.175	0.877
Putative UDP-glucuronate decarboxylase	AT2G28760	-0.074	0.893	0.077	0.570	-0.049	0.098	-0.042	-0.071	-0.252	-0.383	0.506	0.873

Calmodulin-like protein	AT3G10190	-0.131	-0.038	-0.354	0.128	0.636	1.003	-0.836	-0.642	-0.511	-0.201	0.165	0.867
Phloem calmodulin-like-domain protein	AT2G17290	0.298	0.186	0.197	0.527	0.411	0.426	0.270	0.027	0.143	0.087	0.595	0.859
Secretory carrier membrane protein	AT1G61250	0.157	0.005	-0.014	0.022	0.188	0.429	-0.015	-0.019	0.033	0.180	0.306	0.851
Cytochrome P450 monooxygenase CYP9	AT2G40890	0.225	0.505	0.417	1.251	-0.526	-0.305	-0.393	-0.457	0.128	0.110	1.239	0.850
Glyceraldehyde-3-phosphate dehydroge	AT3G04120	0.035	0.333	-0.426	0.097	0.036	0.097	0.431	0.221	0.336	0.707	0.834	0.842
At1g30270/F12P21_6	AT1G30270	0.673	0.774	0.692	1.017	0.098	-0.014	0.753	0.497	0.652	0.545	1.544	0.836
Zinc transporter, putative	AT1G55910	0.725	0.229	0.781	0.625	0.568	0.290	0.022	0.201	0.403	0.246	1.115	0.833
Hypersensitive-induced response protei	AT5G62740	-0.355	-0.320	0.118	0.293	0.246	1.123	-0.392	0.074	-0.187	0.091	0.034	0.831
Cystinosin homolog	AT5G40670	0.388	1.192	0.647	1.104	0.145	-0.368	0.076	0.086	-0.105	0.576	1.132	0.827
Fructose-bisphosphate aldolase	AT2G36460	-0.243	-0.023	-0.116	0.099	-0.250	-0.040	-0.207	-0.075	-0.239	0.226	-0.053	0.820
Putative clathrin assembly protein At5g3	AT5G35200	0.120	0.403	-0.078	0.185	0.507	0.593	0.216	0.665	0.216	0.634	0.338	0.817
Receptor-like protein kinase 4	AT4G23180	0.510	0.136	0.006	-0.022	0.729	-0.365	0.554	0.249	0.414	0.353	0.543	0.815
Nuclear transport factor 2	AT1G27970	0.734	0.668	0.362	0.301	1.006	0.708	1.080	1.180	0.995	1.330	1.140	0.815
1,4-benzoquinone reductase-like; Trp re	AT4G27270	-0.283	0.134	0.209	0.240	-0.281	-0.171	-0.663	-0.337	-0.696	-0.412	0.106	0.812
Aconitase-iron regulated protein 1	AT2G05710	0.147	0.394	0.194	0.442	0.173	0.340	0.382	0.147	0.128	0.341	0.531	0.810
AR781	AT2G26530	0.202	0.315	0.473	0.695	0.341	0.505	-0.055	0.667	-0.088	0.661	0.503	0.802
DnaJ homolog subfamily B member 11 p	AT3G62600	-0.229	-0.065	-0.029	0.090	0.169	0.650	-0.097	0.289	0.014	0.359	-0.088	0.801
Putative receptor protein kinase PERK1	AT2G33580	0.384	0.165	0.485	0.308	0.300	0.209	0.240	0.531	0.396	0.675	0.677	0.801
Heat shock cognate 70 kDa protein 3	AT5G02500	0.018	0.247	-0.125	0.154	-0.139	0.281	0.490	0.105	0.505	0.259	0.744	0.794
Caffeic acid 3-O-methyltransferase	AT5G54160	-0.121	-0.365	0.204	-0.111	-0.198	-0.116	0.443	0.255	0.296	0.105	0.735	0.789
Adenosine kinase isoform 1T-like protei	AT5G03300	0.057	0.149	0.475	0.581	-0.068	0.012	0.150	-0.217	0.068	0.032	0.775	0.787
COBRA-like protein 7 precursor	AT4G16120	0.369	0.306	0.771	0.744	0.436	0.263	0.189	0.304	0.213	0.254	1.051	0.786
Ubiquitin-conjugating enzyme E2-17 kDa	AT1G64230	0.533	0.968	-0.164	0.146	0.497	0.506	1.030	1.158	0.866	1.523	0.732	0.785
Reversibly glycosylated polypeptide	AT3G02230	-0.084	-0.044	-0.159	0.283	0.117	0.500	0.451	0.542	0.128	0.242	-0.012	0.775
OSJNBa0058K23.17 protein	AT1G30400	0.206	-2.013	0.459	0.640	-0.072	0.279	-0.277	0.037	-0.134	0.022	0.633	0.766
UPI0000162F22; F26G16.2 protein	AT1G30440	0.557	-0.125	0.042	0.042	0.403	0.386	0.084	-0.103	0.196	0.090	0.627	0.763
Putative heat-shock protein 90	AT4G24190	-0.034	-0.095	-0.255	-0.263	0.046	0.210	0.146	0.026	0.200	0.184	0.144	0.762
Monodehydroascorbate reductase	AT3G52880	0.196	0.075	0.162	0.111	0.187	0.000	0.383	-0.217	0.313	-0.023	0.357	0.750
Aconitate hydratase, cytoplasmic	AT4G35830	-0.010	0.218	0.416	0.621	0.307	0.087	0.203	0.222	0.327	0.361	0.321	0.749
no_annotation_available	AT1G27190	0.469	0.267	0.235	0.291	0.403	0.443	0.558	0.434	0.391	0.434	0.612	0.748
27k vesicle-associated membrane protei	AT4G21450	0.098	0.141	0.157	0.370	0.103	0.208	0.038	0.287	0.011	0.288	0.291	0.743
Aconitase-iron regulated protein 1	AT2G05710	-0.074	0.294	0.222	0.479	0.022	0.280	-0.073	0.184	-0.063	0.050	0.488	0.742
Polyubiquitin	AT4G05320	-0.018	0.233	-0.003	0.232	-0.027	-0.011	0.348	0.134	0.438	0.422	0.379	0.739
Reticuline oxidase-like protein	AT4G20840	-0.429	0.179	0.160	0.859	-0.935	-0.592	-0.220	0.240	-0.421	0.278	-0.349	0.738
Mitochondrial phosphate transporter	AT5G14040	0.259	0.227	-0.007	0.344	-0.140	0.197	0.049	-0.190	-0.335	-0.135	0.075	0.733
Wall-associated kinase 4	AT1G21210	1.736	0.210	1.496	-0.009	1.844	0.187	1.589	0.135	1.630	0.266	1.962	0.726
Plastidic glucose 6-phosphate/phosphat	AT1G61800	0.534	0.036	0.464	0.530	0.302	0.277	-0.059	0.047	-0.192	0.051	0.287	0.723
Adenylate kinase B	AT5G50370	0.206	0.107	0.151	0.040	0.184	0.085	0.344	0.207	0.330	0.217	0.403	0.723
Glucose-6-phosphate/phosphate-translc	AT1G61800	0.246	0.269	0.605	0.543	-0.132	0.050	-0.203	-0.088	-0.296	-0.236	0.362	0.719
Metal transport protein	AT1G05300	0.140	-0.641	0.651	0.128	0.852	0.650	0.129	-0.325	0.130	-0.185	0.604	0.714
Gb AAF07369.1	AT1G63830	-0.057	0.153	0.007	0.196	0.137	0.431	-0.024	-0.014	-0.071	0.154	0.239	0.713
Polyubiquitin	AT5G03240	-0.141	0.155	-0.182	0.122	-0.210	0.113	-0.057	-0.109	-0.177	0.112	0.054	0.710

Multidrug resistance-associated protein	AT2G34660	0.321	-0.061	0.372	-0.066	0.455	0.453	0.113	0.000	0.077	0.006	0.304	0.700
G protein beta subunit	AT4G34460	0.278	0.195	-0.040	0.137	0.428	0.025	0.438	0.114	0.369	0.328	0.556	0.697
40S ribosomal protein S8	AT5G20290	0.254	0.208	0.009	0.004	0.268	0.390	0.599	0.596	0.543	0.786	0.261	0.694
Steroid membrane binding protein, puta	AT3G48890	0.152	0.296	0.278	0.202	0.181	0.362	0.447	0.313	0.517	0.590	0.497	0.687
Luminal-binding protein 1 precursor	AT5G42020	-0.173	-0.140	-0.312	-0.245	0.001	-0.238	0.712	-0.336	0.555	0.129	0.562	0.687
Patellin 1	AT1G72160	0.135	0.534	0.165	0.390	0.223	0.138	-0.008	0.683	0.432	0.940	1.235	0.685
60S ribosomal protein L40	AT3G52590	-0.156	0.230	-0.146	0.284	-0.152	0.055	0.236	0.062	0.232	0.163	0.518	0.685
SNAP25 homologous protein SNAP33	AT5G61210	0.070	-0.065	0.313	0.231	0.094	0.327	-0.087	0.020	-0.055	0.038	0.184	0.683
Ubiquitin and ribosomal protein S27a,	AT2G47110	-0.149	0.281	-0.010	0.231	-0.133	0.028	0.267	0.031	0.300	0.317	0.598	0.682
Serine/threonine/tyrosine kinase	AT2G24360	0.188	0.060	0.089	0.109	0.226	0.137	0.248	-0.148	0.166	0.049	0.421	0.681
TOM (Target of myb1)-like protein	AT5G16880	-0.141	0.119	-0.039	0.237	0.094	0.261	0.285	0.206	-0.032	0.226	0.175	0.679
Alcohol dehydrogenase	AT1G77120	0.199	0.162	0.237	0.189	0.427	0.008	0.776	0.470	1.014	0.888	0.387	0.678
At1g66480	AT1G66480	0.386	0.164	-0.022	0.104	0.129	0.222	0.321	0.252	0.372	0.409	0.435	0.677
F22C12.16	AT1G64080	-0.051	-0.220	-0.081	-0.062	-0.194	0.135	-0.329	-0.056	-0.177	0.512	-0.227	0.677
Putative phytoalkaline kinase receptor precu	AT2G02220	1.718	0.323	1.939	-0.195	2.056	0.217	2.203	0.233	2.047	0.049	2.264	0.672
Cinnamyl alcohol dehydrogenase	AT5G19440	0.258	0.398	0.459	0.700	0.195	0.290	0.370	0.389	0.524	0.547	0.611	0.666
F15H18.11	AT1G18390	0.538	0.685	0.424	0.728	0.337	0.403	0.811	0.522	0.848	0.726	1.038	0.664
T23K8.15 protein	AT1G65240	0.364	0.350	0.181	0.263	0.309	0.298	0.563	0.382	0.462	0.836	0.383	0.661
Polyubiquitin	AT5G20620	-0.174	-0.017	-0.123	0.042	-0.209	0.029	0.093	-0.072	-0.106	0.090	0.249	0.660
Enolase 1	AT2G36530	-0.115	0.220	0.075	0.379	0.110	0.301	0.306	0.213	0.197	0.462	0.246	0.656
Heat shock cognate 70 kDa protein 3	AT3G12580	0.031	0.352	-0.195	0.153	-0.061	0.084	0.555	0.151	0.552	0.321	0.454	0.656
P58IPK	AT5G03160	-0.112	0.245	0.361	0.144	-0.167	0.093	-0.020	0.072	0.004	0.305	0.431	0.652
At1g65020	AT1G65020	-0.244	0.239	-0.328	0.157	0.046	0.484	0.180	0.430	0.202	0.507	0.170	0.651
Ras-related GTP-binding protein	AT5G45130	-0.108	0.126	-0.038	0.112	-0.038	0.040	-0.302	-0.156	-0.406	-0.096	0.355	0.651
Caffeic acid O-methyltransferase	AT5G54160	0.308	0.219	0.435	0.243	0.091	-0.034	-0.365	-0.157	-1.059	-0.079	0.957	0.650
Mitochondrial carrier-like protein	AT4G01100	0.605	0.548	0.305	0.648	0.535	0.425	0.546	0.251	0.419	0.462	0.864	0.646
SDL12A	AT5G42080	0.082	0.628	0.010	0.393	0.026	0.264	0.314	0.404	0.066	0.551	0.338	0.642
Syntaxin 121	AT3G11820	-0.102	0.076	0.393	0.711	-0.113	0.220	-0.913	0.117	-0.746	0.160	0.320	0.640
T13M11.15 protein	AT1G61790	0.062	0.211	-0.022	0.086	0.052	0.499	-0.093	0.109	-0.179	0.102	0.013	0.633
Receptor-like protein kinase	AT2G31880	0.023	0.402	0.098	0.530	-0.092	0.171	-0.178	0.214	-0.176	0.336	0.026	0.629
prolyl 4-hydroxylase, beta polypeptide	AT5G60640	0.088	0.044	0.398	0.298	-0.031	-0.014	-0.341	-0.023	-0.142	0.063	0.237	0.628
DnaJ-like protein Msl1	AT3G44110	0.202	0.153	-0.331	0.169	0.544	0.479	0.532	0.173	0.492	0.584	0.545	0.627
UPI000009CD7E; P0401G10.6	AT4G24290	0.209	0.301	0.028	0.231	-0.025	0.335	0.447	0.278	0.255	0.533	0.399	0.620
Synaptobrevin-like protein	AT1G04760	0.183	0.315	0.084	0.090	0.276	0.646	0.299	0.659	0.197	0.604	0.220	0.619
F9F8.20 protein	AT3G10980	0.071	0.107	0.348	0.317	-0.053	-0.174	-0.050	0.296	-0.161	0.226	-0.031	0.617
SDL12A	AT5G42080	0.356	0.453	-0.113	0.349	-	0.187	0.077	0.371	-	0.665	0.338	0.606
Eugenol O-methyltransferase	AT5G54160	0.789	-0.236	0.455	-0.407	0.751	-0.260	0.151	-0.420	0.584	-0.126	0.955	0.606
At2g18730/MSF3.11	AT2G18730	0.346	0.107	0.446	0.022	0.504	0.562	0.983	0.576	0.797	0.885	0.770	0.604
Amt2-like protein	AT2G38290	0.089	0.212	-0.094	0.074	0.170	0.304	-0.218	-0.012	-0.259	0.074	0.175	0.595
Hexose transporter	AT5G26340	0.030	0.290	-0.095	0.257	-0.197	0.169	-0.521	-0.431	-0.549	-0.223	0.135	0.592
Receptor-like serine/threonine kinase	AT1G70530	0.380	0.344	-0.171	0.218	0.299	0.410	0.312	0.462	0.286	0.469	0.101	0.584
AT3g28670/MZN14_13	AT3G28670	0.110	0.069	0.134	0.083	0.248	-0.764	0.206	-0.074	-0.088	-0.015	0.240	0.582

Cytosolic ascorbate peroxidase	AT1G07890	0.082	0.143	-0.179	-0.219	-0.002	0.079	0.268	0.549	0.182	0.498	0.361	0.581
Polyubiquitin	AT5G20620	-0.033	0.249	0.110	0.178	-0.111	-0.078	0.286	0.044	0.365	0.356	0.510	0.581
Putative membrane transporter	AT2G26510	0.349	0.357	0.122	0.211	0.170	0.169	0.327	0.057	0.183	0.364	0.727	0.580
Erwinia induced protein 1	AT2G17120	0.040	0.078	0.184	-0.102	0.447	0.319	0.561	0.272	0.178	0.300	0.539	0.579
F8L10.9 protein	AT1G53050	-0.178	-0.018	0.128	0.311	-0.004	0.172	-0.481	-0.138	-0.333	-0.104	0.400	0.579
Sucrose synthase	AT3G43190	0.129	0.061	0.077	-0.094	0.207	0.324	0.298	0.087	0.185	0.213	0.418	0.573
14-3-3 protein	AT5G16050	-0.016	0.262	-0.131	0.141	-0.169	-0.128	0.038	-0.145	-0.049	0.041	0.385	0.573
14-3-3-like protein D	AT2G42590	-0.011	0.271	0.165	0.244	0.104	-0.029	0.221	0.128	0.163	0.193	0.645	0.572
40S ribosomal protein S7	AT1G48830	0.053	0.081	0.073	0.256	0.006	0.263	-0.026	0.174	-0.120	0.119	0.071	0.570
AT4g34700/T4L20_280	AT4G34700	0.276	0.219	0.119	0.248	0.042	0.122	0.283	0.298	0.160	0.173	0.211	0.568
Heat shock 70 kDa protein	AT3G12580	0.236	0.022	0.055	0.036	0.124	0.356	0.569	0.316	0.700	0.273	0.485	0.568
Aluminum-induced protein	AT5G19140	0.544	0.646	0.516	0.790	0.717	0.415	0.712	0.805	0.828	1.044	0.942	0.567
UBC protein	AT4G05320	-0.182	0.032	-0.100	-0.015	-0.243	-0.008	0.003	-0.028	0.021	-0.145	0.295	0.567
T24D18.14 protein	AT1G16030	-0.147	0.168	-0.301	0.048	-0.070	0.077	0.544	0.160	0.356	0.352	0.439	0.565
Disulfide-isomerase-like protein	AT2G47470	0.194	-0.235	0.061	-0.013	-0.255	-0.616	0.315	-0.533	0.335	-0.264	0.466	0.561
Cytosolic phosphoglycerate kinase 1	AT1G79550	0.169	0.108	0.069	0.191	0.172	0.068	0.369	-0.034	0.267	0.209	0.258	0.549
S-adenosyl-L-methionine synthetase 1	AT3G17390	0.080	0.157	0.363	0.675	-0.162	0.059	-0.143	-0.047	-0.350	0.003	0.867	0.545
AtPK2324	AT2G48010	0.320	0.270	0.225	0.377	0.106	-0.003	0.207	0.073	0.154	0.216	0.742	0.544
Glutamine synthetase	AT5G37600	0.124	0.362	0.740	0.854	-0.154	0.183	-0.408	-0.021	-0.415	-0.188	0.051	0.540
ATP synthase delta chain, mitochondrial	AT5G13450	-0.067	0.083	0.141	0.124	-0.066	-0.008	0.114	-0.099	-0.023	-0.149	0.221	0.540
Putative aluminum-induced protein	AT3G22850	-0.212	0.026	-0.031	-0.080	-0.300	-0.181	-0.364	-0.352	-0.525	-0.501	-0.015	0.537
AT5g36940/MLF18_60	AT1G58030	-0.002	0.168	-0.098	0.150	0.370	-0.162	0.403	-0.029	-0.012	0.342	0.448	0.536
Ribosomal protein L10, putative	AT1G66580	0.112	0.075	0.052	0.302	0.150	0.354	-0.198	0.037	-0.076	0.060	0.007	0.531
F3O9.32 protein	AT1G16520	0.121	0.318	0.145	0.326	0.117	0.132	0.432	0.323	0.269	0.395	0.604	0.523
no_annotation_available	AT5G40450	0.376	0.462	0.485	1.375	0.041	-0.190	-0.120	0.140	-0.122	0.280	1.173	0.521
Pectinesterase-like protein	AT5G48450	0.056	0.490	-0.155	0.256	0.285	0.496	0.219	0.687	-0.667	0.587	0.410	0.519
Putative ripening regulated protein	AT5G52450	0.214	0.491	0.363	0.670	-0.210	0.134	-0.177	0.291	-0.012	0.082	0.302	0.517
UDP-glucose:sterol 3-O-glucosyltransfer	AT3G07020	0.118	-0.374	0.575	0.006	0.115	0.436	0.643	0.440	0.651	0.429	0.132	0.503
Leucine-rich repeat protein, putative	AT4G35470	-0.270	0.317	-0.187	0.416	0.402	0.358	0.258	0.554	0.010	0.499	0.243	0.498
Putative elongation factor 1 gamma	AT1G57720	0.390	0.352	-0.095	0.104	0.329	0.281	0.482	0.209	0.308	0.606	0.447	0.497
Putative peroxisomal membrane carrier	AT2G39970	0.028	0.124	0.163	0.372	-0.260	-0.058	-0.237	-0.127	-0.330	-0.329	-0.052	0.494
Allyl alcohol dehydrogenase	AT5G16990	0.062	-0.282	0.136	-0.072	0.167	0.302	0.552	0.109	0.596	0.166	-0.004	0.490
Actin-11	AT5G09810	0.079	0.463	0.156	0.364	-0.105	0.048	0.228	0.260	0.020	0.428	0.495	0.489
Zinc finger, C3HC4 type, putative	AT5G22000	0.181	0.053	0.019	0.012	0.624	0.391	0.329	0.053	0.252	0.149	0.287	0.489
Polyubiquitin	AT4G05320	-0.273	-0.046	-0.047	0.023	-0.261	-0.025	-0.162	-0.114	-0.131	-0.150	0.147	0.486
14-3-3-like protein	AT1G78300	0.384	0.185	0.074	-0.022	0.297	0.082	0.394	0.189	0.303	0.703	0.464	0.483
RE10554p	AT3G52590	-0.135	0.130	-0.253	0.034	-0.206	0.078	-0.132	-0.092	-0.231	-0.008	-0.046	0.482
F10O3.10 protein	AT1G03080	0.035	0.601	0.019	0.406	-0.049	0.015	0.076	0.326	-0.108	0.157	0.304	0.482
Protein At1g23170	AT1G70770	0.007	0.169	-0.176	0.287	-0.026	0.135	0.048	0.185	0.022	0.255	0.084	0.482
SF16 protein-like	AT2G33990	0.093	0.012	0.074	0.101	0.019	0.124	-0.207	-0.122	-0.298	0.061	0.384	0.475
YUP8H12.24 protein	AT1G05150	-0.097	-0.184	0.048	0.010	-0.786	0.158	-0.763	0.165	-0.861	0.311	-1.029	0.471
OSJNBb0022F16.9 protein	AT1G78830	0.102	-0.145	0.148	-0.006	0.344	0.156	0.474	0.014	0.353	0.021	0.582	0.469

Ribosomal protein L40	AT3G52590	0.328	0.280	0.364	0.390	0.036	0.221	0.119	0.240	0.224	0.375	0.318	0.466
Polyubiquitin	AT4G02890	-0.102	0.236	0.056	0.101	0.008	0.157	0.271	0.205	0.324	0.255	0.562	0.465
Putative iron inhibited ABC transporter	AT5G60790	0.343	0.826	-0.036	0.504	0.081	0.249	0.104	0.269	0.152	0.310	0.442	0.464
Patellin-3	AT1G72160	0.012	0.393	0.042	0.322	0.169	0.292	-0.317	0.257	-0.077	0.296	0.174	0.463
Protein kinase APK1A, chloroplast precu	AT1G07570	0.094	-0.088	0.284	0.154	0.387	0.510	0.321	0.385	0.305	0.345	0.384	0.461
Putative receptor-like protein kinase	AT1G34300	0.027	0.227	0.101	0.280	0.197	0.154	-0.046	0.199	0.136	0.247	0.323	0.458
T14P8.16	AT4G02350	0.069	0.147	-0.017	0.420	0.084	0.028	0.210	0.364	0.185	0.211	0.303	0.457
Ubiquitin	AT2G47110	-0.215	0.125	-0.242	-0.004	-0.301	-0.065	-0.211	-0.198	-0.246	0.098	0.193	0.456
UTP:alpha-D-glucose-1-phosphate uridy	AT5G17310	0.039	0.122	0.161	0.179	-0.042	0.250	0.401	0.397	-0.037	0.071	0.191	0.456
Sterol delta-7 reductase	AT1G50430	0.263	0.122	0.408	0.279	0.110	0.065	0.136	-0.157	0.079	-0.035	0.605	0.453
Triosephosphate isomerase	AT3G55440	0.035	0.072	-0.013	0.062	-0.207	-0.024	-0.016	-0.171	-0.188	-0.055	0.030	0.451
Emb CAB83315.1	AT5G03540	0.125	0.211	-0.010	0.126	0.100	0.011	0.079	0.024	0.082	-0.028	0.154	0.448
Protein kinase APK1B, chloroplast precu	AT2G28930	0.254	0.143	0.124	0.244	0.200	0.308	0.135	0.339	0.084	0.285	0.348	0.446
Putative phragmoplastin	AT3G60190	0.415	-0.289	-0.044	-0.083	0.161	0.258	0.341	0.385	0.388	0.341	0.157	0.446
Receptor-protein kinase-like protein	AT3G51550	0.386	-0.293	0.407	0.001	0.466	0.332	0.852	0.249	0.934	0.248	-0.141	0.444
Translationally-controlled tumor protein	AT3G16640	0.189	0.409	0.084	0.149	0.416	0.435	0.490	0.844	0.418	1.219	0.249	0.442
NADH:cytochrome b5 reductase	AT5G17770	0.123	-0.007	0.231	0.190	0.037	0.036	0.178	-0.078	0.240	0.137	0.398	0.442
Whitefly-induced gp91-phox	AT5G47910	-0.191	-0.141	0.182	-0.060	-0.185	-0.107	0.299	0.341	0.075	0.129	-0.005	0.442
Copine III-like	AT5G14420	0.002	0.261	0.223	0.596	-0.293	-0.012	-0.707	-0.178	-0.723	-0.339	0.342	0.436
UPI00009DA03; putative GTP-binding p	AT4G17530	-0.072	0.103	0.266	0.415	-0.293	-0.305	-0.285	-0.278	-0.271	-0.120	0.433	0.433
Putative UDP-N-acetylglucosamine trans	AT4G32270	0.132	0.062	-0.013	0.140	0.017	0.123	-0.143	0.084	-0.122	0.090	0.193	0.428
40S ribosomal protein S24	AT3G04920	0.211	0.158	0.359	0.111	-0.038	0.281	0.250	0.421	0.099	0.146	0.220	0.427
Polyubiquitin	AT1G31340	-0.249	0.058	0.011	-0.001	-0.254	-0.075	-0.010	-0.067	-0.004	0.118	0.366	0.424
Proton pump interactor	AT4G27500	0.484	0.226	0.183	0.116	0.143	0.124	0.505	0.328	0.536	0.357	0.538	0.419
Calcineurin B-like	AT4G33000	-0.111	0.110	-0.166	0.218	0.243	0.568	0.099	0.380	0.027	0.400	0.507	0.418
40S ribosomal protein S4	AT5G07090	0.101	0.180	-0.175	0.069	0.082	0.289	0.148	0.001	-0.077	0.226	0.077	0.418
Small GTP-binding protein	AT1G02130	-0.031	0.138	0.122	0.302	-0.205	-0.426	-0.139	0.002	-0.234	-0.111	0.278	0.417
Syntaxin 132	AT5G08080	0.154	0.175	0.124	0.261	0.234	0.343	-0.168	0.098	-0.080	0.050	0.003	0.416
F6N23.9 protein	AT4G00710	0.148	0.488	0.248	0.621	0.429	0.464	0.374	0.753	0.390	0.839	0.623	0.415
Ankyrin-like protein	AT2G31820	0.289	0.543	0.299	0.442	-0.217	-0.049	-0.332	-0.016	-0.307	0.055	0.381	0.413
Putative dolichyl-di-phosphooligosaccha	AT5G66680	0.047	0.102	-0.281	-0.073	-0.033	0.049	0.031	-0.292	-0.093	-0.030	-0.006	0.412
Nucleoside diphosphate kinase 1	AT4G09320	0.189	-0.108	0.386	0.072	-0.065	0.249	0.254	0.275	0.200	0.339	0.244	0.411
PDR6 ABC transporter	AT2G36380	0.174	0.497	0.107	0.461	0.362	0.686	0.043	0.636	-0.214	0.645	-0.127	0.410
F6F9.12 protein	AT1G19835	0.530	-0.302	0.281	-0.176	0.598	0.388	0.752	0.435	0.907	0.789	0.703	0.409
Putative Clathrin coat assembly protein	AT5G46630	0.050	0.083	-0.001	0.108	0.074	0.073	0.507	0.247	0.417	0.062	0.546	0.405
Cyclic nucleotide-gated ion channel 1	AT5G53130	0.116	-0.030	-0.070	-0.116	0.498	0.367	0.388	0.128	0.302	0.146	0.389	0.402
Ankyrin-like protein; 93648-91299	AT3G12360	0.027	0.400	-0.081	0.157	0.195	0.213	0.352	0.113	0.200	0.283	0.483	0.396
LysM receptor-like kinase	AT3G21630	-0.063	0.081	-0.068	0.158	-0.180	0.040	-0.227	0.116	-0.213	0.058	0.153	0.396
VDAC1.3	AT3G01280	-0.152	-0.118	0.223	0.072	-0.199	-0.199	-0.028	-0.295	-0.114	-0.218	0.085	0.393
Proteasome subunit beta type 1	AT3G60820	-0.190	-0.057	-0.029	0.032	-0.347	-0.274	-0.210	-0.423	-0.465	-0.529	0.047	0.391
Histidine amino acid transporter	AT5G40780	0.106	-0.218	0.007	0.057	0.156	0.051	0.256	-0.252	-0.440	-0.368	-0.093	0.381
UPI0000196B24; ATP binding / kinase/ p	AT5G01950	0.270	0.038	-0.108	-0.082	0.432	0.081	0.293	0.048	0.152	-0.124	0.558	0.381

Acetyl-CoA acyltransferase	AT2G33150	0.053	-0.053	-0.128	-0.066	-0.192	0.008	-0.280	-0.229	-0.400	-0.334	-0.056	0.379
Putative carbonyl reductase	AT3G61220	-0.082	-0.074	-0.165	0.243	-0.067	-0.303	0.592	0.021	0.586	0.273	0.625	0.379
KUP-related potassium transporter	AT2G30070	0.197	0.500	-0.107	0.131	0.127	0.448	0.388	0.937	0.403	0.848	0.177	0.376
Vesicle-associated membrane protein 7	AT4G15780	-0.089	0.091	0.231	0.027	0.301	0.334	0.103	0.427	0.256	0.397	0.319	0.370
Protein kinase-like protein	AT2G24360	0.304	0.024	0.048	-0.070	0.046	-0.067	0.466	-0.066	0.318	0.082	0.419	0.369
Mitochondrial-processing peptidase alp1	AT3G16480	0.171	0.098	0.256	0.199	0.050	0.089	0.187	-0.033	0.200	0.066	0.248	0.368
Plasma membrane H+ ATPase	AT2G24520	0.225	0.189	0.748	0.302	-0.160	-0.091	-0.100	-0.254	0.074	-0.037	0.080	0.367
Expressed protein	AT2G41705	0.002	0.077	0.083	-0.137	0.203	0.130	0.314	0.050	0.149	0.019	0.231	0.367
F21H2.4 protein	AT1G34750	0.037	0.169	0.103	0.351	0.207	0.256	-0.022	0.037	-0.137	-0.019	0.114	0.361
Arabidopsis thaliana genomic DNA, chro	AT4G27450	-0.177	-0.047	-0.331	0.059	0.074	0.107	0.078	0.392	0.246	0.655	0.178	0.361
F23M19.3	AT1G34320	-0.017	-0.019	-0.087	0.077	0.048	-0.018	0.179	0.075	0.181	0.482	0.202	0.357
Syntaxin 132	AT5G08080	-0.005	0.094	0.177	0.201	0.105	0.236	0.130	0.240	0.002	0.091	-0.028	0.351
Serine hydroxymethyltransferase, mitoc	AT4G37930	-0.023	0.109	0.185	0.345	-0.159	-0.097	-0.065	0.014	0.125	0.185	0.512	0.350
Gb AAF01580.1	AT5G08440	-0.396	0.136	-0.361	0.434	-0.068	-1.152	-0.258	0.037	-0.231	-0.035	-0.016	0.349
Similarity to kinesin protein	AT3G16630	0.114	0.360	0.283	0.185	0.093	0.297	0.304	0.404	0.293	0.305	0.468	0.342
Cysteine synthase (EC 2.5.1.47) (Beta-py	AT4G14880	-0.145	-0.098	-0.096	0.142	0.049	0.097	-0.269	-0.165	-0.129	-0.171	-0.005	0.342
T14P4.10 protein	AT4G02075	0.193	-0.027	0.211	0.284	0.046	0.076	-	0.143	0.120	0.138	0.182	0.341
Zinc finger, C3HC4 type, putative	AT5G22000	-0.016	0.080	0.014	0.129	0.018	0.129	-0.174	0.095	-0.115	0.177	0.348	0.341
Probable 26S proteasome non-ATPase r	AT4G24820	-0.059	0.062	0.038	0.060	0.024	-0.020	-0.132	-0.220	-0.100	-0.223	0.149	0.339
F8K4.10 protein	AT1G61900	0.001	-0.174	0.150	-0.124	0.115	0.204	0.238	0.077	0.114	0.190	0.299	0.331
F2D10.25	AT1G20760	0.050	0.097	0.093	0.036	0.240	0.224	0.425	0.115	0.452	0.416	0.471	0.330
Protein kinase CDG1-like	AT5G56890	0.034	0.041	0.273	0.122	0.030	0.025	-0.036	-0.008	0.073	-0.109	0.318	0.329
Ser-thr protein kinase	AT2G40270	0.137	-0.062	0.099	0.152	-0.023	-0.020	-0.130	-0.117	0.106	-0.078	0.507	0.326
ADP,ATP carrier protein 1, mitochondria	AT5G13490	0.259	0.029	0.118	0.211	0.186	0.309	0.190	0.002	0.020	-0.043	0.103	0.322
60S ribosomal protein L5	AT3G25520	0.030	0.219	-0.217	0.176	0.117	0.234	0.469	0.207	0.074	0.187	0.290	0.320
Receptor protein kinase-like	AT3G46290	0.225	0.289	0.097	0.144	0.311	0.035	0.626	0.547	0.589	0.649	0.672	0.317
Calcium-dependent protein kinase 8	AT5G19450	-0.134	-0.242	0.016	0.201	-0.361	-0.066	-0.067	0.014	0.009	-0.158	0.094	0.314
Putative receptor-like protein kinase	AT2G01210	0.334	0.317	0.364	0.189	0.411	0.283	0.472	0.565	0.403	0.559	0.393	0.312
Squamosa promoter-binding-like proteir	AT1G76580	0.019	0.071	0.073	0.203	0.271	0.401	0.336	0.173	0.287	0.191	0.325	0.307
OSJNBa0091D06.14 protein	AT1G62740	0.322	0.271	0.102	0.273	0.059	0.102	0.071	0.143	0.095	0.322	0.172	0.297
Transthyretin-like protein	AT5G58220	0.112	0.170	0.051	0.083	0.088	-0.077	0.156	0.066	0.128	0.226	0.185	0.293
Proteasome subunit beta type 3-A	AT1G21720	0.246	0.020	0.354	0.142	-0.132	-0.069	0.028	-0.090	-0.135	-0.231	0.070	0.289
Steroid 5-alpha reductase	AT3G55360	0.233	0.102	0.009	-0.026	0.137	-0.197	0.295	0.036	0.069	0.259	0.244	0.287
Putative mitogen-activated protein kina:	AT4G29810	0.098	-0.003	0.103	0.046	0.261	0.201	0.132	-0.079	0.118	0.084	0.275	0.286
Putative S-phase specific ribosomal prot	AT4G34670	-0.022	0.233	-0.456	0.185	-2.098	0.130	0.115	0.226	0.187	0.319	0.030	0.286
Putative NTS2 protein	AT1G34470	0.002	-0.156	-0.088	-0.070	-0.228	-0.303	-0.019	-0.327	0.035	-0.202	0.376	0.277
F25I16.1 protein	AT1G18650	0.183	0.383	0.352	0.311	-0.168	-0.121	0.067	0.049	0.130	0.309	0.163	0.275
AP2/EREBP transcription factor ERF-2	AT3G16770	0.167	0.720	-0.265	0.137	0.095	0.337	0.265	0.639	0.329	0.716	0.482	0.265
Peroxisomal 2,4-dienoyl-CoA reductase	AT3G12800	-0.448	-0.254	-0.117	0.165	-0.698	-0.562	-0.535	-0.697	-0.664	-0.539	-0.296	0.265
Formate--tetrahydrofolate ligase	AT1G50480	-0.389	-0.033	-0.247	0.029	-0.501	-0.247	-0.547	-0.173	-0.572	-0.204	0.379	0.261
Arabidopsis thaliana genomic DNA, chro	AT3G26090	0.009	0.141	0.219	0.023	0.062	0.043	-0.012	0.019	0.176	0.032	0.358	0.260
Putative carbonyl reductase	AT3G61220	-0.046	-0.193	-0.253	0.160	0.025	-0.244	0.592	-0.024	0.658	0.119	0.679	0.251

40S ribosomal protein S33, putative	AT5G03850	0.468	0.016	0.349	0.117	-0.128	-0.014	-0.085	-0.093	-0.108	-0.016	0.070	0.250
Pectinesterase-3 precursor	AT1G53840	-0.325	-0.107	-0.108	-0.088	-0.137	-0.052	-0.027	0.011	-0.065	0.017	0.039	0.246
Armadillo repeat-containing protein-like	AT1G20780	-0.019	-0.051	0.123	0.028	0.196	0.254	-0.003	0.062	0.192	0.078	0.077	0.224
Latex-abundant protein	AT1G79340	0.027	0.187	0.025	0.188	0.130	-0.061	0.427	0.142	0.346	0.310	0.157	0.201
Glutamate dehydrogenase 2	AT5G07440	-0.242	0.109	0.045	0.292	-0.099	0.333	-0.105	0.361	-0.047	0.276	-0.207	0.160

Table S3. Fold changes (log2) in expression of oxidative stress-related genes in the flavedo (F) and albedo (A) tissues of AC, EC and 1-MCP-treated fruits stored for 4 and 14 days at 20 °C as compared to freshly harvested (FH) fruit. The symbol + indicates no expression in FH fruits, and the symbol -, indicates expression in FH fruits but not in the compared treatment. Numbers in bold indicate differential expression in the compared condition according to SAM (p -value<0.01).

Citrus unigen	Description	4 days						14 days					
		AC		EC		1-MCP		AC		EC		1-MCP	
		F	A	F	A	F	A	F	A	F	A	F	A
Glutathione S-transferase/Glutathione peroxidase													
aC18011D05Rv_c	Glutathione S-transferase	0.246	0.459	0.254	0.464	0.199	0.008	0.118	-0.141	-0.048	-0.138	1.069	4.646
aC31502H06EF_c	Glutathione S-transferase	0.290	0.074	0.127	0.223	0.577	1.342	0.249	-0.100	0.425	0.366	1.051	3.802
aCL184Contig2	Glutathione S-transferase	0.351	0.617	0.357	0.556	0.327	0.064	0.289	-0.154	0.053	-0.140	1.178	3.667
aCL184Contig1	Glutathione S-transferase	0.364	0.425	0.414	0.483	0.504	-0.071	0.221	-0.363	0.337	-0.223	1.383	2.896
aCL3761Contig1	Glutathione S-transferase	0.767	0.185	1.664	0.697	1.317	1.508	0.342	0.484	0.584	0.236	1.398	2.618
aC31704E06EF_c	Glutathione S-transferase	0.802	0.322	0.908	0.430	0.869	0.748	0.329	0.277	0.517	0.355	1.274	2.270
aC34105C06EF_c	Glutathione S-transferase	0.859	-0.105	1.416	0.533	1.024	1.107	0.248	0.081	0.460	0.253	1.142	2.214
aCL110Contig2	Glutathione S-transferase		0.225	+	-	-		-		-		0.684	2.058
aC05811E06SK_c	Glutathione S-transferase 12	0.500	0.601	-0.620	-0.837	0.143	-0.420	0.395	0.781	0.511	0.645	0.904	1.569
aCL1507Contig2	Glutathione S-transferase GST 14	0.164	0.141	0.096	0.039	0.274	0.265	0.120	-0.002	0.121	0.055	0.913	1.429
aCL1249Contig1	Glutathione S-transferase GST 14	0.341	0.518	0.442	0.603	0.714	1.034	0.352	0.485	0.306	0.347	0.916	1.393
aCL4064Contig1	Glutathione S-transferase GST 14	0.709	0.608	0.560	0.619	0.955	0.905	0.529	0.355	0.459	0.326	0.588	1.325
aC31303F07EF_c	Glutathione S-transferase GST 22	0.384	1.034	0.263	1.068	0.887	1.501	0.129	0.866	0.031	0.858	0.433	1.057
aC16016H02SK_c	Glutathione S-transferase	0.029	0.077	0.021	0.113	0.095	0.065	-0.160	-0.082	0.010	0.033	0.267	0.839
aC08034B04SK_c	Glutathione S-transferase GST 22	0.523	1.369	0.429	1.424	1.345	1.891	0.537	1.195	0.445	1.143	0.265	0.653
aCL7288Contig1	Glutathione S-transferase GST 22	0.532	1.036	0.288	1.063	1.166	1.423	0.549	0.768	0.467	0.920	0.817	0.467
aC06017H12SK_c	Glutathione S-transferase zeta class	0.120	-0.051	0.189	0.084	0.132	0.152	0.242	0.102	0.299	-0.013	0.282	0.338
aCL3279Contig1	Glutathione S-transferase zeta class	0.291	0.104	0.231	0.174	0.314	0.053	0.055	-0.108	0.176	0.053	0.174	0.240
aCL4101Contig1	Glutathione S-transferase, C-terminal-like	0.384	0.675	0.583	0.856	-0.222	-0.213	0.224	0.007	0.254	0.016	0.834	0.223
aC31304H09EF_c	Putative glutathione S-transferase T3	0.252	0.173	0.552	0.540	1.068	1.158	0.111	0.381	0.202	0.654	-0.282	-0.175
aCL1099Contig1	Similarity to glutathione-S-transferase/glutaredoxin	0.032	-0.094	0.060	-0.036	-0.100	-0.048	-0.080	-0.078	-0.049	-0.080	-0.407	-0.951
aC20007C12SK_c	Glutathione S-transferase	0.061	-0.071	0.041	0.020	0.109	-1.288	0.266	0.215	0.132	0.159	+	-
Blue copper oxidases													
aCL3449Contig1	Dicyanin	0.480	0.023	2.493	1.564	-0.098	1.176	-0.353	0.199	0.671	0.432	2.052	2.960
aCL12Contig4	Dicyanin	-0.070	0.114	0.830	1.270	0.222	1.483	-1.174	0.147	-0.909	0.407	0.553	2.835
aCL5752Contig1	Dicyanin	0.115	0.111	0.791	-0.008	0.359	0.294	0.499	0.308	-1.174	0.458	0.696	0.740

Citrus unigen	Description	4 days						14 days					
		AC		EC		1-MCP		AC		EC		1-MCP	
		F	A	F	A	F	A	F	A	F	A	F	A
Ascorbate-gluthatione cycle and related													
aCL622Contig2	Cationic peroxidase isozyme 40K precursor	-0.278	+	0.160	+	-	+	-0.054	+	0.062	+	0.326	+
aCL47Contig2	Ascorbate peroxidase	0.521	0.000	0.597	0.056	0.610	0.738	0.670	0.325	0.802	0.890	1.500	2.382
aC31401A05EF_c	Phospholipid hydroperoxide glutathione peroxidase	0.146	0.226	0.470	0.528	0.133	0.170	-0.208	0.074	-0.087	0.108	0.477	1.366
aCL2220Contig3	Class III peroxidase	0.089	0.766	0.356	0.284	-0.050	1.415	0.109	0.848	0.805	1.065	-0.071	0.926
aCL14Contig2	Fe-superoxide dismutase 1	0.285	0.012	0.078	-0.119	0.447	0.348	0.559	0.180	0.605	0.504	0.381	0.867
aCL8011Contig1	Fe-superoxide dismutase 1	0.435	-0.031	0.255	0.035	0.586	0.347	0.392	0.166	0.588	0.389	0.516	0.827
aCL1534Contig1	Peroxidase	0.307	-0.345	0.557	-0.141	0.144	-0.364	0.002	-0.132	0.717	0.122	1.132	0.776
aC31302C03EF_c	Monodehydroascorbate reductase	0.196	0.075	0.162	0.111	0.187	0.000	0.383	-0.217	0.313	-0.023	0.357	0.750
aCL1413Contig1	Glutathione reductase, cytosolic	-0.389	0.006	0.011	0.402	-0.573	-0.269	-0.650	-0.427	-0.612	-0.397	-0.244	0.587
aCL5500Contig1	Cytosolic ascorbate peroxidase	0.082	0.143	-0.179	-0.219	-0.002	0.079	0.268	0.549	0.182	0.498	0.361	0.581
aCL277Contig1	Chloroplast thylakoid-bound ascorbate peroxidase	0.047	0.035	-0.004	0.028	-0.116	-0.141	0.070	-0.110	-0.203	0.073	0.435	0.576
aCL2981Contig2	Lactoylglutathione lyase	0.110	-0.098	-0.131	-0.165	0.386	0.385	0.509	-0.012	0.333	-0.018	0.467	0.570
aC31101F04EF_c	Peroxidase 21 precursor	0.762	0.907	0.864	0.370	0.995	0.381	1.128	0.773	0.886	0.662	1.266	0.518
aCL8529Contig1	Peroxidase precursor	0.135	-0.284	0.902	0.174	0.099	0.038	0.083	0.032	0.477	-0.030	1.015	0.461
aCL7572Contig1	Cu-Zn superoxide dismutase	-0.155	0.079	-0.684	-0.499	-0.272	0.082	-0.045	-0.049	0.133	-0.131	0.251	0.125
aC31003C03EF_c	Catalase	-0.264	-0.427	-0.610	-0.847	-0.188	-0.370	-0.049	-0.376	-0.183	0.011	-0.115	-0.207
aCL3047Contig2	Cu/Zn superoxide dismutase	0.029	0.310	0.111	0.192	0.750	0.292	-0.101	0.644	0.037	0.333	0.088	-0.307
aCL74Contig2	Phospholipid hydroperoxide glutathione peroxidase	-0.318	-0.566	-0.391	-0.927	-0.370	-0.396	0.179	-0.252	0.120	-0.117	-0.767	-0.318
aCL63Contig3	Catalase	-0.295	-0.517	-0.423	-0.894	-0.121	-0.303	-0.222	-0.368	-0.238	-0.152	-0.340	-0.385
aCL3047Contig1	Cu/Zn superoxide dismutase	-0.432	0.532	0.040	0.185	0.015	0.039	-0.672	0.781	-0.477	0.417	-0.286	-0.408
aCL2220Contig2	Class III peroxidase	0.194	-0.313	0.478	-0.138	-0.156	-0.396	0.378	-0.131	0.354	-0.321	-0.065	-0.482
aCL8723Contig1	Putative sodium-dependent bile acid symporter	-0.032	-0.121	-0.845	-0.529	0.278	-0.468	0.595	-0.213	0.494	0.032	0.093	-0.531
aCL193Contig1	Dehydroascorbate reductase	-0.118	-0.291	-0.340	-0.262	-0.007	0.157	-0.350	-0.226	-0.253	-0.122	-0.506	-0.561
aCL1389Contig1	Glutathione reductase	0.095	-0.011	0.756	0.245	-0.854	-0.875	-0.397	-0.703	-0.688	-0.524	0.323	-0.694
aCL3818Contig1	Monodehydroascorbate reductase	-0.301	-0.024	-0.818	-0.693	-0.047	0.084	-0.282	-0.518	-0.731	-0.894	-0.506	-0.781
aC31305D02EF_c	Cu/Zn superoxide dismutase	-0.949	1.009	-0.487	0.641	-0.129	0.240	-0.980	1.256	-0.831	1.060	-0.434	-1.286
aCL36Contig2	Peroxidase precursor	-0.414	-0.009	-1.509	-0.912	0.755	0.146	0.372	0.180	-1.232	-0.748	-2.354	-2.275
aC08032B11SK_c	Peroxidase precursor	0.085	-	0.206	-	-	-	-	-	0.597	0.316	-	-

Citrus unigen	Description	4 days						14 days					
		AC		EC		1-MCP		AC		EC		1-MCP	
		F	A	F	A	F	A	F	A	F	A	F	A
Thioredoxin-dependent pathway_redoxin													
aC08015E04SK_c	Thioredoxin	-0.143	+	0.316	+	-0.048	+	-0.089	+	-0.153	+	0.179	+
aCL8673Contig1	Thioredoxin M-type 3, chloroplast precursor	-0.019	+	0.653	+	-0.046	+	-2.240	+	0.199	+	0.282	+
aCL709Contig1	Thioredoxin reductase 1	0.265	-0.167	0.632	0.537	-0.028	-0.390	0.209	0.288	0.090	0.338	0.524	1.091
aC07002C08SK_c	UPI000034F380; Glutaredoxin-like protein	-0.150	-0.307	0.104	0.008	0.122	0.392	-0.164	-0.135	-0.081	-0.013	0.935	1.076
aCL5456Contig1	Glutaredoxin-related-like protein	0.052	0.407	-0.110	0.157	-0.114	0.230	-0.024	-0.060	-0.011	0.240	0.322	0.813
aCL5576Contig1	Glutaredoxin-related-like protein	0.285	0.493	0.042	0.331	0.254	0.162	-0.030	0.019	-0.051	0.219	0.304	0.782
aC08008G07SK_c	Thioredoxin H	-0.348	-0.464	0.204	0.241	-0.400	-0.141	-1.100	-0.535	-0.978	-0.548	-0.894	0.710
aC08011E03SK_c	Thioredoxin X, chloroplast precursor	-0.224	0.235	0.133	0.234	-0.089	0.146	0.186	0.227	0.325	0.199	0.479	0.394
aCL18Contig3	Thioredoxin H	-0.202	0.017	0.120	0.267	-0.440	-0.129	-0.588	-0.333	-0.665	-0.248	-0.223	0.292
aCL4011Contig1	Thioredoxin X, chloroplast precursor	-0.242	-0.934	-1.172	-1.057	0.367	0.116	0.609	-0.393	0.523	-0.209	-0.519	-0.160
aCL130Contig3	Glutaredoxin	-0.374	-0.336	-0.350	-0.430	-0.391	-0.381	-0.983	-0.587	-0.756	-0.609	-0.682	-0.251
aCL4509Contig1	Chloroplast thioredoxin M-type	0.048	-0.134	-0.079	-0.017	-0.050	-0.021	-0.222	-0.088	-0.097	-0.193	-0.352	-0.258
aCL2621Contig1	Glutaredoxin precursor	-0.097	-0.158	-0.179	0.037	-0.261	-0.066	-0.179	-0.143	-0.266	-0.242	-0.534	-0.288
aCL6997Contig1	Putative glutaredoxin	-0.200	-0.150	-0.228	-0.258	-0.286	-1.160	-0.465	-0.159	-0.434	-0.258	-0.537	-0.432
aCL1978Contig1	Thioredoxin F-type, chloroplast precursor	-1.039	-0.887	-1.472	-0.959	-1.265	-0.774	-0.824	-0.577	-0.922	-0.704	-0.941	-0.541
aCL1232Contig1	Putative thioredoxin m2	-0.125	0.075	-0.129	-0.138	-0.040	-0.010	0.206	-0.159	0.060	-0.021	-0.179	-0.576
aC08001H10SK_c	Thioredoxin family Trp26-like protein	0.103	0.495	-0.695	-0.757	-0.078	-0.142	0.382	0.769	0.585	0.662	-0.447	-0.689
aCL3764Contig1	Ferredoxin-thioredoxin-reductase catalytic subunit B precursor	-0.303	-0.183	-0.457	-0.353	-0.706	-0.519	-0.442	-0.290	-0.666	-0.526	-0.894	-0.742
aCL149Contig1	Thioredoxin H-type	-0.289	-0.356	-0.301	-0.621	-0.616	-0.881	-0.459	-0.853	-0.678	-0.701	-0.519	-1.265
aC07008A11SK_c	Thioredoxin-like 5, chloroplast precursor	-0.612	-0.861	-0.728	-1.047	-0.160	-0.679	-0.607	-0.556	-0.602	-0.526	-1.283	-1.442
Miscellaneous													
aC08027E03SK_c	Nectarin 5	0.180	2.112	1.167	3.157	0.828	3.400	-2.829	1.816	-0.975	1.572	1.017	5.469
aCL1084Contig1	CPRD2 protein	0.741	0.534	1.607	1.330	0.585	0.992	-0.335	0.168	0.284	0.350	1.906	3.696
aCL494Contig3	Glycolate oxidase	0.082	0.000	0.021	0.242	0.247	0.438	-0.008	-0.109	-0.184	0.113	0.951	1.711
aCL5192Contig1	Putative short-chain acyl-CoA oxidase	0.030	-0.269	-0.156	0.144	0.161	-0.138	0.031	-0.218	0.071	-0.242	0.603	1.245
aC08018H06SK_c	Urate oxidase	0.489	0.946	0.881	1.171	0.568	0.090	0.979	1.246	1.498	1.463	1.473	1.184
aC01017A05SK_c	Amine oxidase	0.188	0.898	-0.296	0.550	0.704	0.404	0.823	0.852	0.744	1.156	1.125	1.060
aC31105C08EF_c	Acyl-coenzyme A oxidase 4, peroxisomal	-0.016	-0.155	0.031	0.025	0.120	-0.099	-0.045	-0.126	-0.017	-0.214	0.550	0.938
aCL784Contig1	Reticuline oxidase-like protein (berberine)	-0.429	0.179	0.160	0.859	-0.935	-0.592	-0.220	0.240	-0.421	0.278	-0.349	0.738
aCL4451Contig1	Zeta-carotene desaturase	0.119	0.230	0.093	0.337	-0.045	0.084	0.313	0.370	0.288	0.206	0.144	-0.437
aCL35Contig1	Beta carotene hydroxylase	0.579	1.008	0.337	0.639	-0.354	-0.327	0.188	-0.047	-0.146	0.317	0.252	-0.565
aCL3421Contig1	Zeaxanthin epoxidase	0.121	0.507	0.095	0.360	-0.445	-0.751	0.135	-0.315	0.126	-0.128	-0.434	-0.841
aC07010E12SK_c	Copper amine oxidase, putative	-0.555	-0.311	-0.537	-0.591	-0.537	-0.720	-0.661	-0.741	-0.598	-0.635	-0.735	-1.057
aCL1551Contig1	Zeaxanthin epoxidase	-0.005	0.671	-0.052	0.425	-0.755	-0.841	-0.254	-0.456	-0.285	-0.329	-0.684	-1.160
aC31706A07EF_c	Zeaxanthin epoxidase	-0.249	0.486	-0.262	0.341	-0.935	-1.244	-0.217	-0.538	-0.300	-0.353	-0.485	-1.331